

Figure 6.1: Photoluminescence spectra from  $\text{Si}_{1-x-y}\text{Ge}_x\text{C}_y$  samples with  $x = 0.38$  and various  $[\text{C}]$ . The pump power density was  $\sim 50 \text{ W/cm}^2$ . The spectra were normalized and corrected to account for the spectral response of the experimental optical path.

sample. The low-energy edge was used to avoid complications arising from band filling. We estimate error bars of  $\pm 6$  meV for the absolute band gap but only  $\pm 2$  meV for the relative band gaps. The change in band gap with respect to that of the C-free samples is plotted as a function of C fraction in Fig. 6.2. This data showed that  $\Delta E_G/\Delta y = +21 \pm 2$  meV/%C, in near agreement with previous PL results[80] which indicated  $+24$  meV/%C for samples with  $x = 0.16$ . These luminescence results were corroborated by Lanzerotti's temperature-dependent collector current measurements on  $\text{Si}_{1-x-y}\text{Ge}_x\text{C}_y$  base heterojunction bipolar transistors fabricated in our lab, which yielded a value of  $+26$  meV/%C for  $x = 0.20$  and  $0.25$ [81].

That the luminescence and electron transport experiments should give the same result for  $\Delta E_G$  is not obvious. The luminescence is due to the recombination of electrons and holes, which will preferentially settle in low  $E_G$  regions; while transport across the base of an HBT requires the electrons to sample the entire width of the base. Thus, we expect PL to measure the lowest band gap region and HBT collector current to measure the average band gap. That the two gave similar results indicated that the band gap of the  $\text{Si}_{1-x-y}\text{Ge}_x\text{C}_y$  was spatially uniform (i.e., the minimum band gap approximately equalled the average band gap).

The substitutional incorporation of C into pseudomorphic  $\text{Si}_{1-x}\text{Ge}_x$  on Si (001) should have two effects on the band gap of the alloy. First, the smaller C atoms will reduce the strain in the film, thus increasing the band gap. Additionally, the presence of C in the matrix should have a separate, intrinsic effect on the band gap of the *relaxed* alloy.

$$\Delta E_{G,total} = \Delta E_{G,strain} + \Delta E_{G,intrinsic} \quad (6.2)$$

The effect of strain reduction can be computed using the standard deformation potential framework[4, 5] as discussed in Chap. 2, if the deformation potentials are known or assumed. For biaxially compressed  $\text{Si}_{1-x}\text{Ge}_x$  and  $\text{Si}_{1-x-y}\text{Ge}_x\text{C}_y$ ,  $\Delta E_{G,strain}$  is given

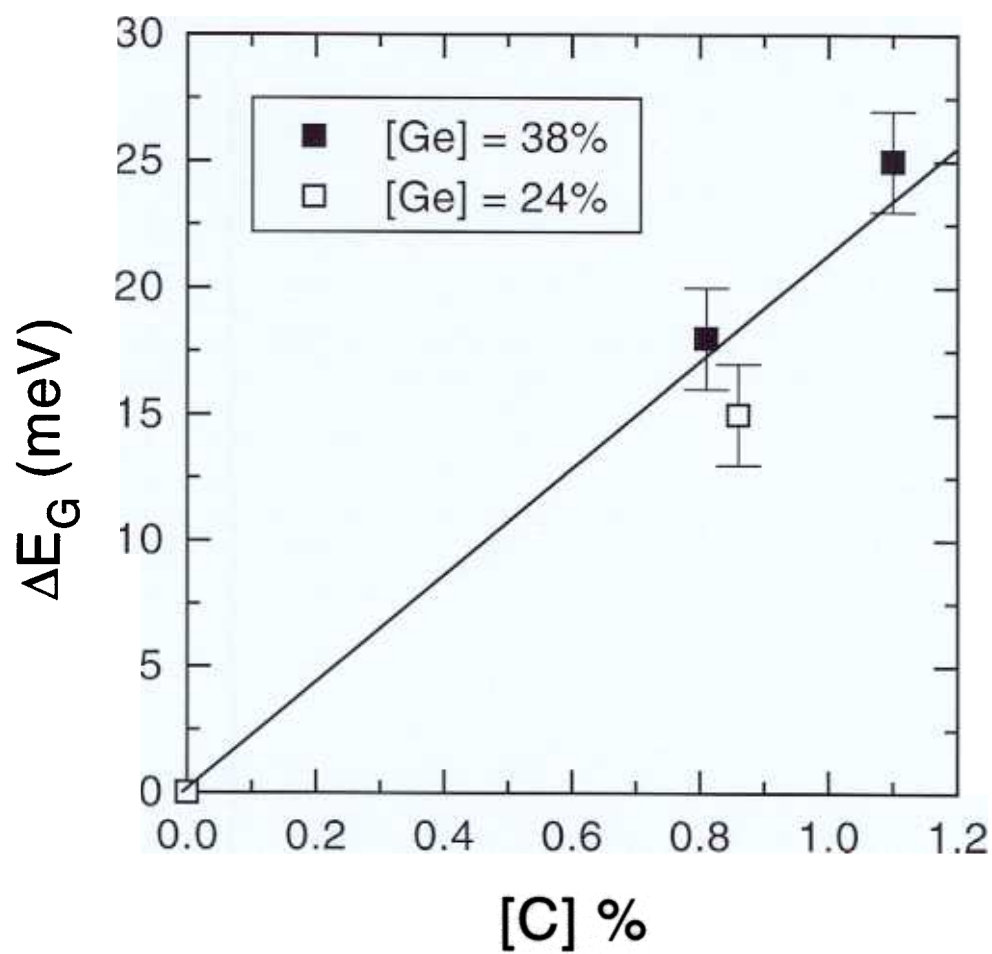


Figure 6.2: Change in band gap of strained  $\text{Si}_{1-x-y}\text{Ge}_x\text{C}_y$  as a function of C fraction.

by

$$\Delta E_{G, \text{strain}} = \left[ \Xi_d + \frac{1}{3} \Xi_u - a_v \right] (2\epsilon_{\parallel} + \epsilon_{\perp}) + \left[ b - \frac{1}{3} \Xi_u \Delta \right] (\epsilon_{\perp} - \epsilon_{\parallel}) \quad (6.3)$$

$$\epsilon_{\perp} = -2 \frac{c_{12}}{c_{11}} \epsilon_{\parallel} \quad (6.4)$$

where the first term in Eqn. 6.3 is due to hydrostatic stress (change in volume, but not shape) and the second to uniaxial stress (change in shape, but not volume), and all of the parameters are generally taken as linear interpolations between the constituent elements of the alloy. For biaxially compressed  $\text{Si}_{1-x-y}\text{Ge}_x\text{C}_y$  on Si (001), Eqn. 6.4 becomes

$$\epsilon_{\perp} = -2 \frac{c_{12}}{c_{11}} [0.042(8.3y - x)] \quad (6.5)$$

assuming that 1 C atom compensates the misfit due to 8.3 Ge atoms.

Using Eqns. 6.3 and 6.5 and linearly interpolated elastic constants, we computed the effect of strain on the band gap for any composition. The result turns out to be almost linear in  $x$  and  $y$  for  $x < 0.4$ , with  $\Delta E_{G, \text{strain}} \approx 11.7\epsilon_{\parallel} = 0.49(8.3y - x)$ . We then subtracted the calculated  $\Delta E_{G, \text{strain}}$  from our measured  $\Delta E_{G, \text{total}}$  to determine the intrinsic effect of C on the band gap of relaxed  $\text{Si}_{1-x-y}\text{Ge}_x\text{C}_y$ . In Fig. 6.3 we have plotted the expected band gap of relaxed  $\text{Si}_{1-x-y}\text{Ge}_x\text{C}_y$  as a function of lattice constant. Note that the relaxed  $\text{Si}_{1-x-y}\text{Ge}_x\text{C}_y$  points lie below the relaxed  $\text{Si}_{1-x}\text{Ge}_x$  line and, more importantly, that their slope is positive ( $\sim +10$  eV/nm). That is, as C is added and the lattice constant decreases, the relaxed band gap does as well (-20 meV/%C). This is slightly surprising in light of the fact that SiC and diamond have band gaps much larger than both Si and  $\text{Si}_{1-x}\text{Ge}_x$ . However, it is not unprecedented; similar “bowing” is observed or predicted in the band gap of other alloy systems which have a large lattice mismatch (e.g., GaAs/GaSb and GaAs/GaN)[82]. Also, Demkov and Sankey[83] predicted that the initial substitutional incorporation of C into relaxed  $\text{Si}_{1-y}\text{C}_y$  would lower the alloy’s band gap. In fact, they even suggested that the material might turn metallic for  $y \approx 10\%$ . Although our experimental results

on  $\text{Si}_{1-x-y}\text{Ge}_x\text{C}_y$  do not match the magnitude of the bowing predicted by Demkov and Sankey, they agree qualitatively and are in clear contradiction with predictions based solely on interpolation between the band structures of Si, Ge, and C or SiC[84].

The previous computation of  $\Delta E_{G,\text{intrinsic}}$  assumed that the deformation potentials in our pseudomorphic  $\text{Si}_{1-x-y}\text{Ge}_x\text{C}_y$  were the same as those in  $\text{Si}_{1-x}\text{Ge}_x$ . However, extrapolating our  $\text{Si}_{1-x-y}\text{Ge}_x\text{C}_y$  data back to zero strain (Fig. 6.4) gives the band gap of relaxed  $\text{Si}_{1-x-y}\text{Ge}_x\text{C}_y$ , without relying on knowledge of its deformation potentials. This can then be compared to the known band gap of the relaxed  $\text{Si}_{1-x}\text{Ge}_x$  alloy[6, 15] with the same Ge content to determine the effect of C on the band gap of relaxed films. Doing so, we found that for *relaxed*  $\text{Si}_{1-x-y}\text{Ge}_x\text{C}_y$ ,  $\Delta E_{G,\text{intrinsic}}/\Delta y = -19 \text{ meV}/\%C$ . That this agrees with the above result (which assumed  $\text{Si}_{1-x}\text{Ge}_x$  deformation potentials) confirms that the deformation potentials of  $\text{Si}_{1-x-y}\text{Ge}_x\text{C}_y$  are indeed similar to those of  $\text{Si}_{1-x}\text{Ge}_x$ .

Brunner *et al.*[50] recently measured photoluminescence from pseudomorphic  $\text{Si}_{1-y}\text{C}_y/\text{Si}$  quantum well structures. Unlike our layers which were under compressive strain, their Ge-free layers were under biaxial tension, which also decreases the band gap. In our  $\text{Si}_{1-x-y}\text{Ge}_x\text{C}_y$  films, increasing  $y$  decreased the magnitude of the strain and consequently increased the band gap. In their  $\text{Si}_{1-y}\text{C}_y$  films, increasing  $y$  increased the magnitude of the strain and decreased the band gap. Their PL peak shift of  $-57 \text{ meV}/\%C$  was corrected for quantum confinement yielding a band gap shift of  $-65 \text{ meV}/\%C$ . Subtracting the effect of the macroscopic strain (similarly to Eqn. 6.3), they calculated an intrinsic band gap reduction due to C of  $-19 \text{ meV}/\%C$ , agreeing exactly with our result for C in relaxed  $\text{Si}_{1-x-y}\text{Ge}_x\text{C}_y$ .

Our PL results assume that the strained  $\text{Si}_{1-x-y}\text{Ge}_x\text{C}_y/\text{Si}$  interface is Type I and that the electrons and holes responsible for the luminescence are in the  $\text{Si}_{1-x-y}\text{Ge}_x\text{C}_y$ . However, it is conceivable that the addition of C significantly raises the conduction band of the  $\text{Si}_{1-x-y}\text{Ge}_x\text{C}_y$  above that of the Si so that the measured luminescence is

actually due to recombination of  $\text{Si}_{1-x-y}\text{Ge}_x\text{C}_y$  valence band holes with Si conduction band electrons. Experiments in our group to measure the band offsets at the  $\text{Si}_{1-x-y}\text{Ge}_x\text{C}_y/\text{Si}$  interface are on-going[85].

### 6.3 Towards Zero Strain

In Fig. 6.4 we have plotted the band gap versus biaxial compressive strain for both pseudomorphic  $\text{Si}_{1-x}\text{Ge}_x$  on Si (001) (adapted from the work of Van de Walle and Martin[4, 5]) and our experimental  $\text{Si}_{1-x-y}\text{Ge}_x\text{C}_y$  data points. The most important point to notice is that all of the  $\text{Si}_{1-x-y}\text{Ge}_x\text{C}_y$  points lie below the  $\text{Si}_{1-x}\text{Ge}_x$  line. As C is added to  $\text{Si}_{1-x}\text{Ge}_x$  and the Ge content is held fixed, the strain decreases and the band gap increases, but the band gap increase is much less than it would be if the strain was reduced simply by removing Ge without adding C. That is, for a given band gap,  $\text{Si}_{1-x-y}\text{Ge}_x\text{C}_y$  has less strain (and presumably a greater critical thickness) than does  $\text{Si}_{1-x}\text{Ge}_x$ . The average slope of the  $\text{Si}_{1-x-y}\text{Ge}_x\text{C}_y$  points,  $\Delta E_G/\Delta \epsilon = -6.1$  eV/unit strain, corresponds to  $\Delta E_G/\Delta y = +21$  meV/%C, assuming that each C atom compensates the strain of 8.3 Ge atoms. Furthermore, if one assumes a linear extrapolation of our  $\text{Si}_{1-x-y}\text{Ge}_x\text{C}_y$  data to zero strain, one predicts a significant band gap offset to Si for strain-free  $\text{Si}_{1-x-y}\text{Ge}_x\text{C}_y$  films. For  $x = 0.38$ , the offset would be  $\sim 190$  meV.

From Fig. 6.4 we can readily see that our  $\text{Si}_{1-x-y}\text{Ge}_x\text{C}_y$  films with about 1% C are only about a third or a quarter of the way to zero strain. Achieving strain-free material with  $x = 0.25-0.35$  requires 3-4% C, and we and others have already seen that material quality degrades and substitutional C content saturates for  $[\text{C}] > \sim 2\%$  for growth techniques such as ours. However, significant improvements in the trade-off between band gap and critical thickness can already be attained without reaching the zero strain condition. For example, we have assumed that the elastic properties

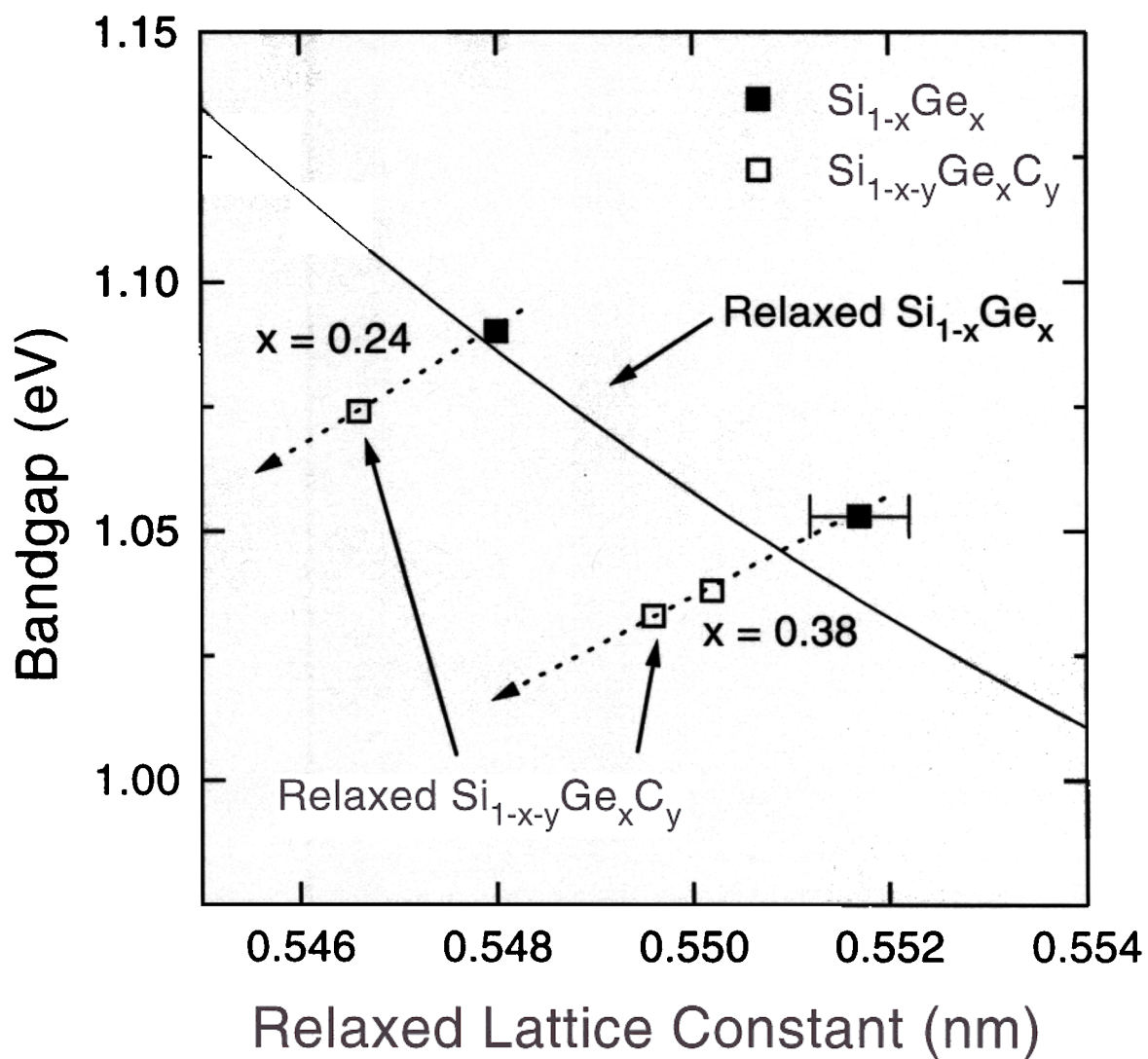


Figure 6.3: Band gap as a function of lattice constant for unstrained material. The  $\text{Si}_{1-x-y}\text{Ge}_x\text{C}_y$  points are adapted from our measurements on pseudomorphic films. For the  $\text{Si}_{1-x}\text{Ge}_x$  line, 15 meV was added to Weber's fit[15] to account for the FE energy.

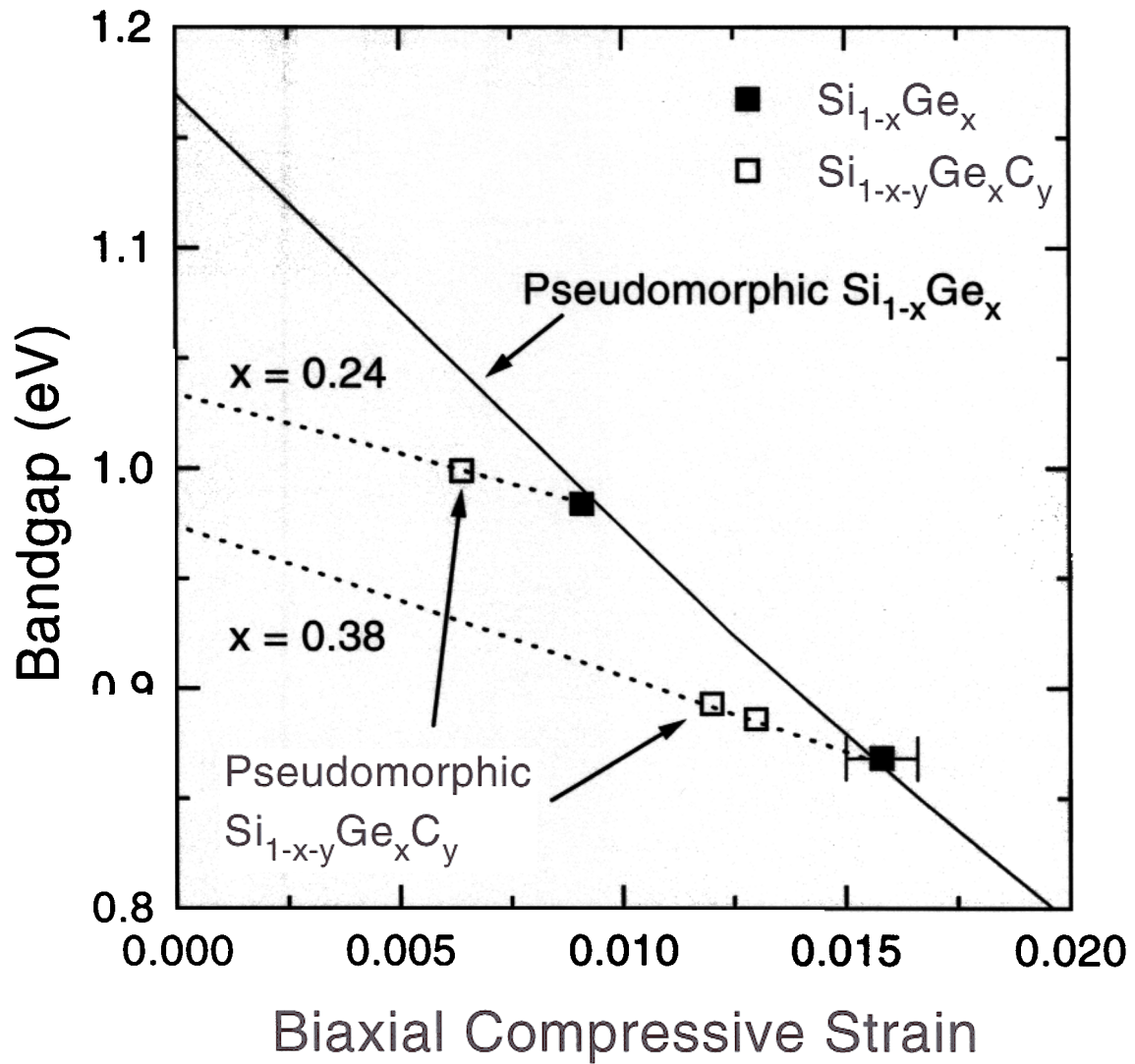


Figure 6.4: Band gap as a function of strain for pseudomorphic films on Si (001). The  $\text{Si}_{1-x}\text{Ge}_x$  line is from Ref. [4].

of  $\text{Si}_{1-x-y}\text{Ge}_x\text{C}_y$  equal those of  $\text{Si}_{1-x}\text{Ge}_x$  and have calculated the Matthews-Blakeslee equilibrium critical thickness for  $\text{Si}_{1-x-y}\text{Ge}_x\text{C}_y$  films (Fig. 6.5). Furthermore, using our measured  $\Delta E_G/\Delta y$ , we can then plot  $h_c$  as a function band gap offset to Si. We have done so in Fig. 6.6 for  $y = 0, 1, 2,$  and  $3\%$ . For large  $x$  and  $y = 0.01$  ( $\Delta E_G > 200$  meV), the improvement is fairly small,  $\sim 30\%$  increase. For  $\Delta E_G = 100$  meV, we predict that the equilibrium critical thickness will increase from about  $260 \text{ \AA}$  to  $660 \text{ \AA}$  for a film with only  $1\%$  C. Because C increases the hardness of Si and  $\text{Si}_{1-x}\text{Ge}_x$ [86], a even larger increase might be expected in the metastable critical thickness.

To demonstrate that adding C to  $\text{Si}_{1-x}\text{Ge}_x$  can indeed increase its critical thickness, we prepared two samples under identical conditions ( $x = 0.38$ ,  $h = 340 \text{ \AA}$ , and capped with  $100 \text{ \AA}$  of Si), except that in one case we added  $1.1\%$  C to the  $\text{Si}_{1-x}\text{Ge}_x$  layer. The sample without C showed luminescence originating from dislocations[19], indicating that the sample was relaxed (Fig. 6.7). The sample with C, however, showed only band-edge,  $\text{Si}_{1-x}\text{Ge}_x$ -like PL with no dislocation lines. Furthermore, defect etching ( $\text{CrO}_3:\text{HF}$  for 5 minutes) revealed many dislocations in the C-free sample, while none were visible in the  $\text{Si}_{1-x-y}\text{Ge}_x\text{C}_y$  sample (Fig. 6.8).

What we have done is trade mechanical instability (strain in  $\text{Si}_{1-x}\text{Ge}_x$ ) for chemical instability (super-saturated substitutional C concentration in  $\text{Si}_{1-x-y}\text{Ge}_x\text{C}_y$ ). And we have found that for this specific thermal budget and composition, the reduced-strain  $\text{Si}_{1-x-y}\text{Ge}_x\text{C}_y$  with super-saturated C was more metastable than was the fully strained  $\text{Si}_{1-x}\text{Ge}_x$ . Further work is needed to completely explore the relative metastability of pseudomorphic  $\text{Si}_{1-x}\text{Ge}_x$  and  $\text{Si}_{1-x-y}\text{Ge}_x\text{C}_y$ .

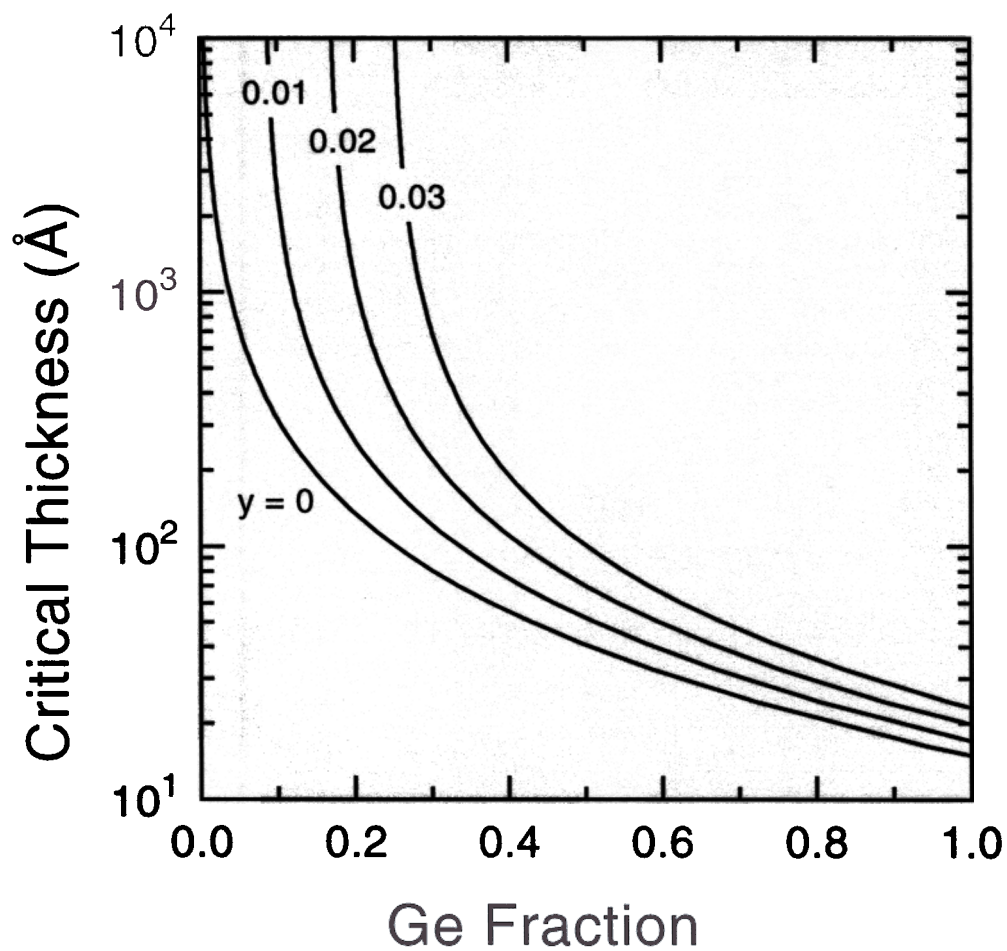


Figure 6.5: Critical thickness of pseudomorphic  $\text{Si}_{1-x-y}\text{Ge}_x\text{C}_y/\text{Si}$  (001). The critical thickness is from the Matthews-Blakeslee equilibrium model, assuming that the elastic properties of  $\text{Si}_{1-x-y}\text{Ge}_x\text{C}_y$  are the same as those of  $\text{Si}_{1-x}\text{Ge}_x$ .

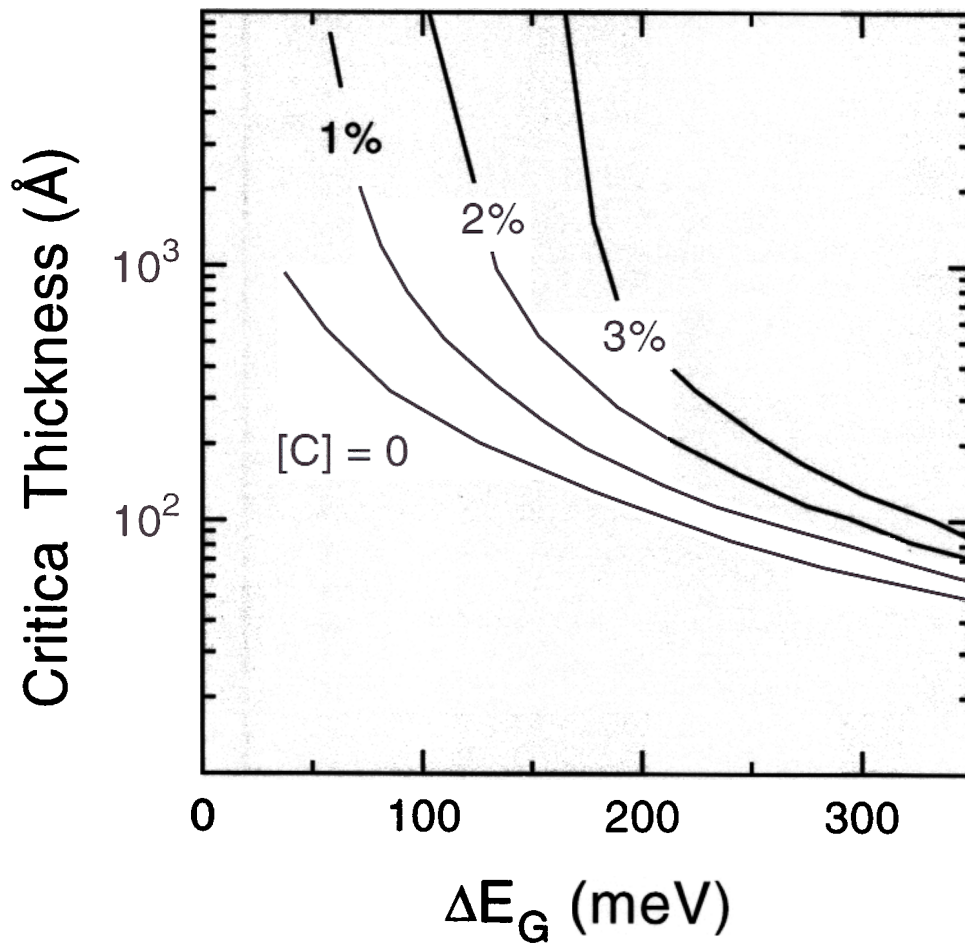


Figure 6.6: Comparison of critical thickness/band gap trade-off for  $\text{Si}_{1-x}\text{Ge}_x$  and for  $\text{Si}_{1-x-y}\text{Ge}_x\text{C}_y$ . The critical thickness is from the Matthews-Blakeslee equilibrium model, assuming that the elastic properties of  $\text{Si}_{1-x-y}\text{Ge}_x\text{C}_y$  are the same as those of  $\text{Si}_{1-x}\text{Ge}_x$ .

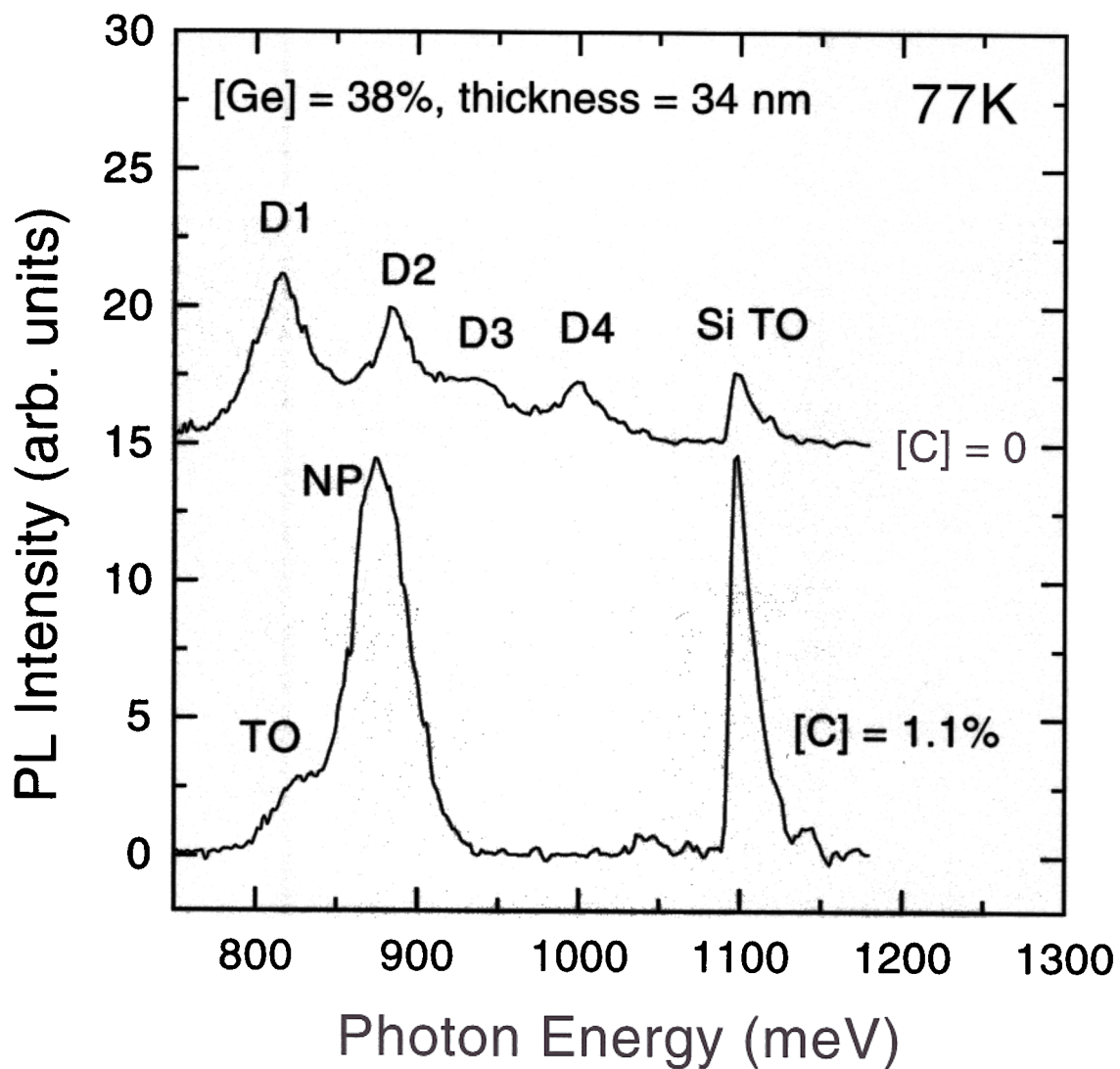


Figure 6.7: Uncorrected photoluminescence spectra for two samples: one with and one without C.

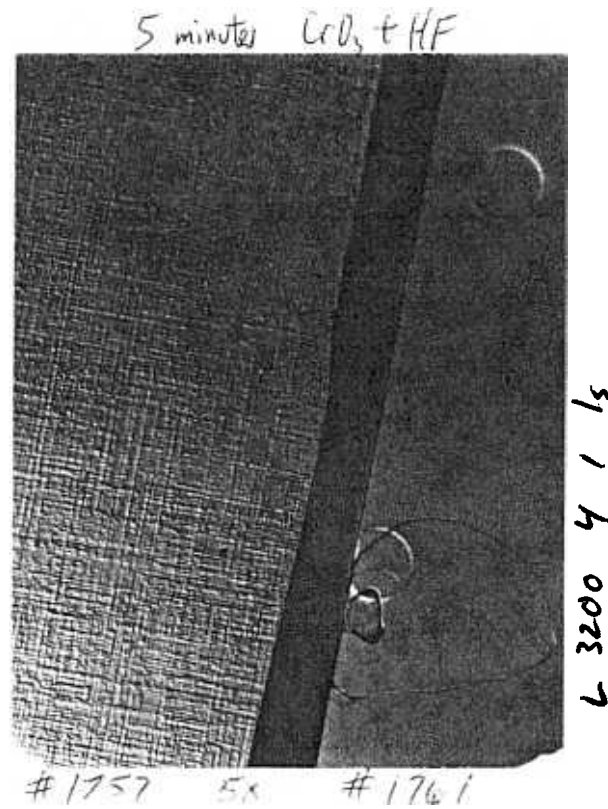


Figure 6.8: Optical photograph of relaxed  $\text{Si}_{1-x}\text{Ge}_x$  (left) and strained  $\text{Si}_{1-x-y}\text{Ge}_x\text{C}_y$  (right). Samples were etched for 5 minutes in 4 HF:5 0.3M  $\text{CrO}_3$  at room temperature. The circles on the  $\text{Si}_{1-x-y}\text{Ge}_x\text{C}_y$  are due to bubbles during the defect etching.

## $\text{Si}_{1-x-y}\text{Ge}_x\text{C}_y$ *p-i-n* Diodes

### 6.4.1 Diode Fabrication

$\text{Si}_{1-x-y}\text{Ge}_x\text{C}_y$  *p-i-n* diodes were fabricated and characterized. The diodes consisted of 560 Å nominally undoped  $\text{Si}_{0.8}\text{Ge}_{0.2}\text{C}_y$  layers sandwiched between *in situ* doped n- and p-type Si. See Fig. 6.9. The  $\text{Si}_{1-x-y}\text{Ge}_x\text{C}_y$  layers were grown at 625°C, and the methylsilane flow was varied from 0 to 0.2 sccm. The diodes were formed by a single-mesa, two-mask process. First, the mesas were plasma etched in  $\text{SF}_6$ , and then the Ti(300 Å)/Al(1200 Å) metallization was patterned by lift-off. The  $\sim 0.5$  μm high mesas were  $180 \times 320$  μm, while the top metal contact was only about a third as to allow optical access from the top surface.

### 6.4.2 Diode I-V

current-voltage characteristics of several ( $\sim 10$ ) randomly selected diodes from each wafer were measured. We compared the geometric mean of the I-V curves from each wafer. These curves are plotted in Fig. 6.10. There was no apparent forward-bias current trend with C concentration; and the forward current ideality factor was approximately 1.8 for all concentrations, indicating that the forward current was primarily due to depletion region recombination rather than to recombination in a neutral region. However, in reverse bias, the leakage current clearly increased and the breakdown voltage decreased with [C]. The C-free control sample and the 0.6% C sample displayed very similar I-V characteristics. The lack of increase in leakage may be an indication that at low C levels there is not a significant increase in recombination/generation centers. However, if the leakage was due to the unpassivated mesa perimeter rather than to the  $\text{Si}_{1-x-y}\text{Ge}_x\text{C}_y$  bulk, nothing can be inferred about the effect of C on the leakage current. (We do not believe this to be the case in that similarly prepared all-Si control devices did not show a size dependence consis-

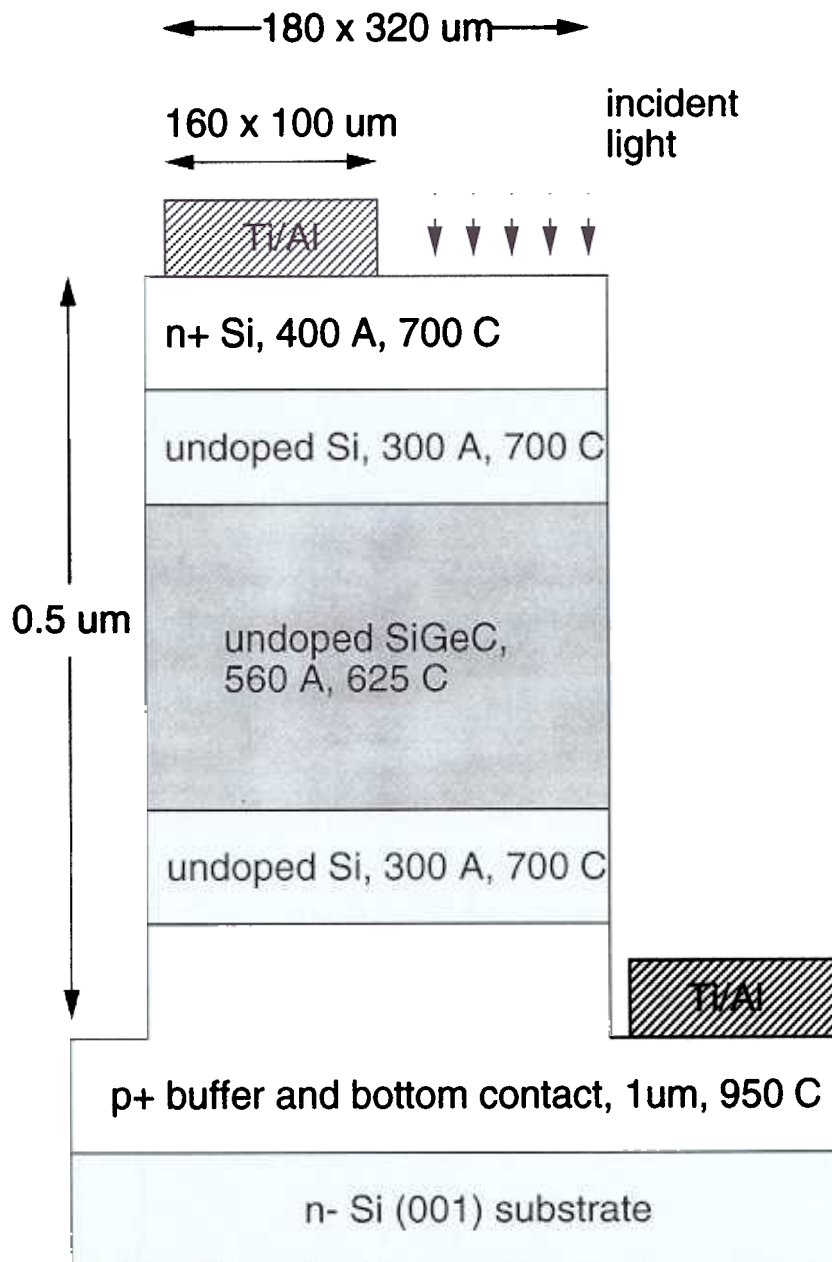


Figure 6.9: Device structure of  $p-i-n$  diodes. The  $p^+$  layer was doped with  $7 \times 10^{18} \text{ cm}^{-3}$  B, and the  $n^+$  layer was doped with  $3 \times 10^{19} \text{ cm}^{-3}$  P. The unintentionally doped region was found by spreading resistance to contain  $\sim 10^{17} \text{ cm}^{-3}$  B.

tent with perimeter leakage.) The diodes with the highest C content (1.2%) were clearly degraded compared to the control sample. The leakage at -3 V, for example, went from  $10^{-4}$  to  $10^{-2}$  A/cm<sup>2</sup>, and the breakdown became much softer and moved from -9 V to  $\sim$ -5 V. Recall that the C concentrations were measured by XRD and that this method assumes that all C atoms are substitutional. The C fraction measured by this means has been shown to saturate at high methylsilane flow, whereas the true  $C_{total}$  might not[79]. In that case, our sample with 1.2% C might contain a large amount of non-substitutional C, which would contribute electrically active generation/recombination centers[54].

At the intermediate C concentration (1.0%), the I-V behavior was bi-modal: the diodes could be split into two groups with very different breakdown characteristics. As can be seen in Fig. 6.11, about a third of the diodes had an I-V curve similar to those at lower [C] but with a somewhat higher leakage current and lower breakdown voltage. The other two-thirds had a significantly lower breakdown voltage ( $\sim$ -6 V). If this lower breakdown voltage was caused by a single "killer defect," the yield of good devices  $Y$ [87] is given by

$$\ln Y = -A \cdot \delta$$

where  $A$  is the device area and  $\delta$  is the defect density. Our case, with  $Y = 0.33$  and  $A = 5.8 \times 10^{-4}$  cm<sup>2</sup>, yields a defect density of  $1.9 \times 10^3$  cm<sup>-2</sup> or an average defect spacing of 460  $\mu\text{m}$ . This large defect spacing is difficult to understand if it is assumed that the defects are interstitial C or SiC precipitates. In both cases, one might expect a greater density of small defects.

#### 6.4.3 Photoresponse

The reverse bias photocurrent of the  $\text{Si}_{1-x-y}\text{Ge}_x\text{C}_y$  diodes was measured. The photoresponse was due to photogeneration of electron-hole pairs. If all of the photogenerated electrons and holes are separated by the electric field and contribute current,

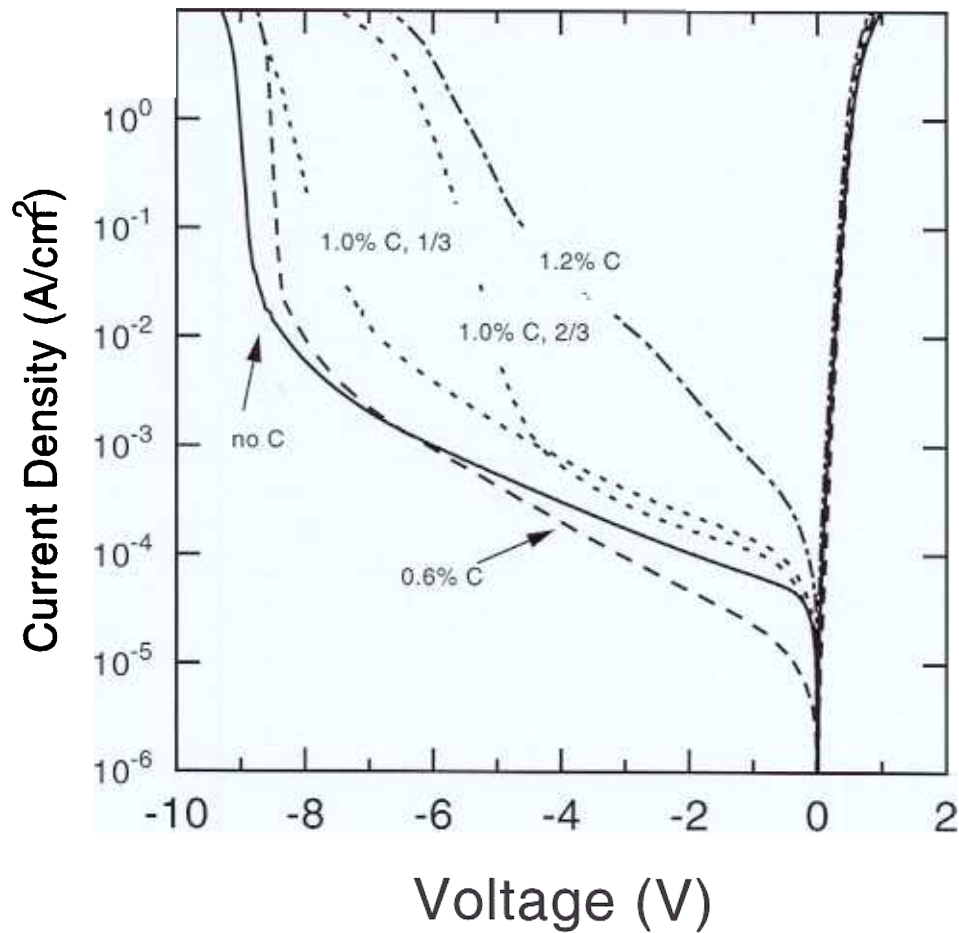


Figure 6.10:  $\text{Si}_{1-x-y}\text{Ge}_x\text{C}_y$  p-i-n diode current-voltage characteristics measured at room temperature.

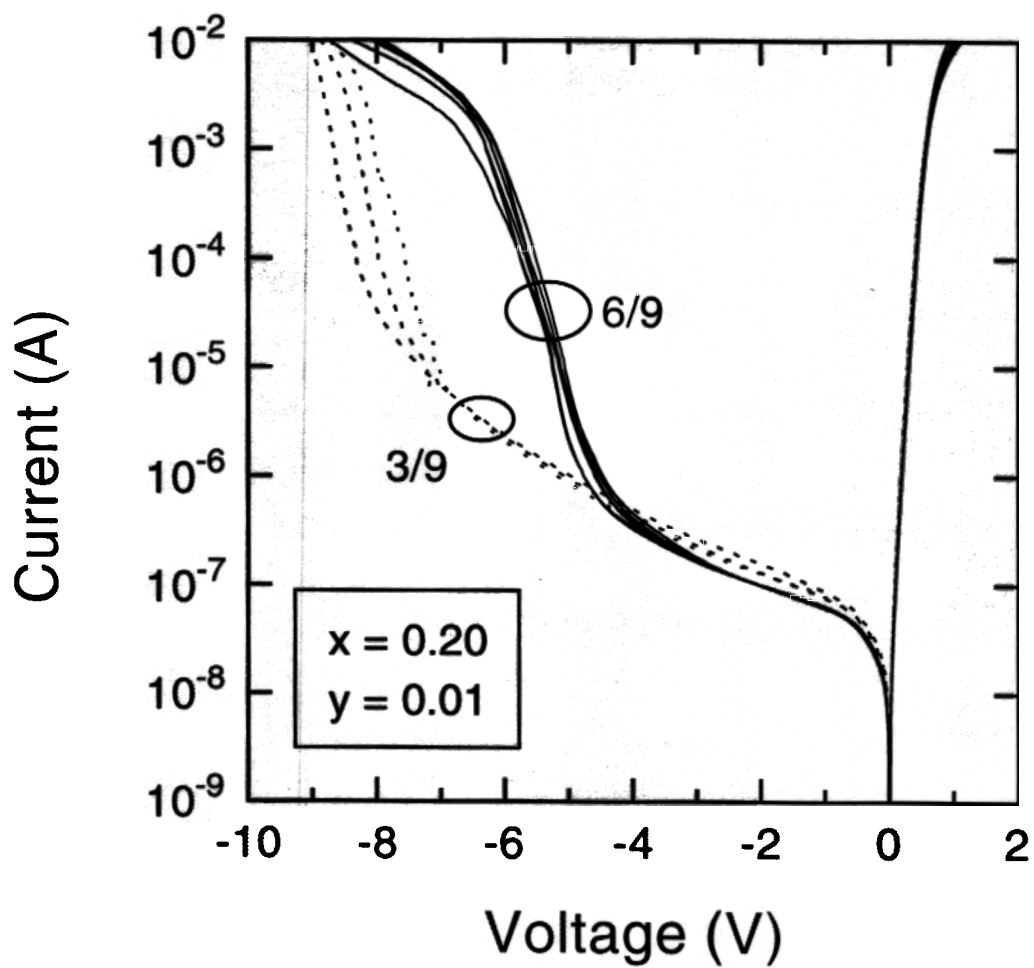


Figure 6.11: Room temperature  $\text{Si}_{1-x-y}\text{Ge}_x\text{C}_y$   $p-i-n$  diode current-voltage characteristics showing bimodal behavior of the devices with 1.0% C.

then the photocurrent  $I_{photo}$  is given by

$$I_{photo}(h\nu) = qa(h\nu)\frac{P(h\nu)}{h\nu}$$

where  $q$  is the electronic charge,  $P$  is the optical power,  $a$  is the absorbance, and  $h\nu$  is the photon energy. If the absorbing layer is thin ( $d\alpha \ll 1$ ), then  $a$  just equals  $d\alpha$ , where  $\alpha$  is the absorption coefficient so that

$$I_{photo}(h\nu) = qd\alpha(h\nu)\frac{P(h\nu)}{h\nu}$$

Band-to-band photon absorption in indirect band gap semiconductors like Si and  $\text{Si}_{1-x}\text{Ge}_x$  is primarily by means of phonon emission and absorption[6]. One expects an additional no-phonon process (as seen in photoluminescence) in  $\text{Si}_{1-x}\text{Ge}_x$ , but it has not yet been experimentally observed. The absorption coefficient is given by the Macfarlane-Roberts expression[88], which for photon energies between  $E_G - \hbar\omega$  and  $E_G + \hbar\omega$  is

$$\alpha(h\nu, T) = A\frac{(h\nu - E_G - \hbar\omega)^2}{1 - e^{-\hbar\omega/kT}}$$

where  $\hbar\omega$  is the phonon energy; and for photon energies greater than  $E_G + \hbar\omega$  is

$$\alpha(h\nu, T) = A\left[\frac{(h\nu - E_G - \hbar\omega)^2}{1 - e^{-\hbar\omega/kT}} + \frac{(h\nu - E_G + \hbar\omega)^2}{e^{\hbar\omega/kT} + 1}\right] \quad (6.10)$$

The photoresponse is the photocurrent divided by the photon flux  $\frac{P}{h\nu}$  and is proportional to the absorption coefficient. In Fig. 6.12 we have plotted the room temperature spectral photoresponse of three  $\text{Si}_{1-x-y}\text{Ge}_x\text{C}_y$  devices and an all-Si control device (same structure but with an all-Si undoped region). At low energy ( $h\nu < 1.3$  eV), the  $\text{Si}_{1-x-y}\text{Ge}_x\text{C}_y$  devices, due to the small band gap material, all exhibited a photoresponse larger than that of the the all-Si device. Furthermore, this data exhibited a trend with C fraction agreeing with the luminescence measurements[73]. As C was added to the  $\text{Si}_{1-x}\text{Ge}_x$ , the photoresponse decreased and shifted towards that of the all-Si device. This trend is consistent with the band gap increasing, and thus

absorption decreasing, with the addition of C. However, a diminished photocurrent could also be due to a lower internal quantum efficiency in the diodes with C.

Extracting the band gap of indirect semiconductors from photoresponse (or absorption) data is most reliably done by plotting the square-root of the photoresponse as a function of photon energy[88, 6]. Doing so for the all-Si device, we found as predicted by Eqns. 6.9 and 6.10 that the square-root of the photoresponse was well fit by two straight line segments. The one corresponding to phonon absorption intersects the energy axis at  $E_G - \hbar\omega$ , and it intersects the other corresponding to phonon emission at  $E_G + \hbar\omega$ . Our fit gives  $E_G - \hbar\omega = 1.03$  eV and  $E_G + \hbar\omega = 1.17$  eV, yielding  $E_G = 1.10$  eV and  $\hbar\omega = 70$  meV, close to the known values for Si of 1.12 eV and 58 meV, respectively.

Figure 6.14 shows the square-root of the photoresponse of three  $\text{Si}_{1-x-y}\text{Ge}_x\text{C}_y$  diodes. This data can not be fit by two straight lines as was done for the all-Si device in Fig. 6.13. While the region above 1.00 eV showed the expected quadratic behavior, the photoresponse did not go to zero at  $E_G - \hbar\omega$  ( $\sim 0.90$  eV) as predicted by Eqn. 6.9. These diodes exhibited excess deep absorption, which increased with the C concentration. We can be reasonably certain that the origin of this excess absorption is electrically active defect states within the band gap, and we can speculate that these defects are related to the presence of C. However, it must be noted that the carbon-free device showed this absorption tail as well, and at least four earlier independent photocurrent experiments on strained  $\text{Si}_{1-x}\text{Ge}_x$  diodes grown by low temperature epitaxy suffered similarly from sub- $E_G$  defect absorption[7, 89, 90, 91]. These observations suggest that although the deep absorption increased four-fold when the C content was raised from 0 to 1.0%, the responsible defects may not be due solely to the presence of C.

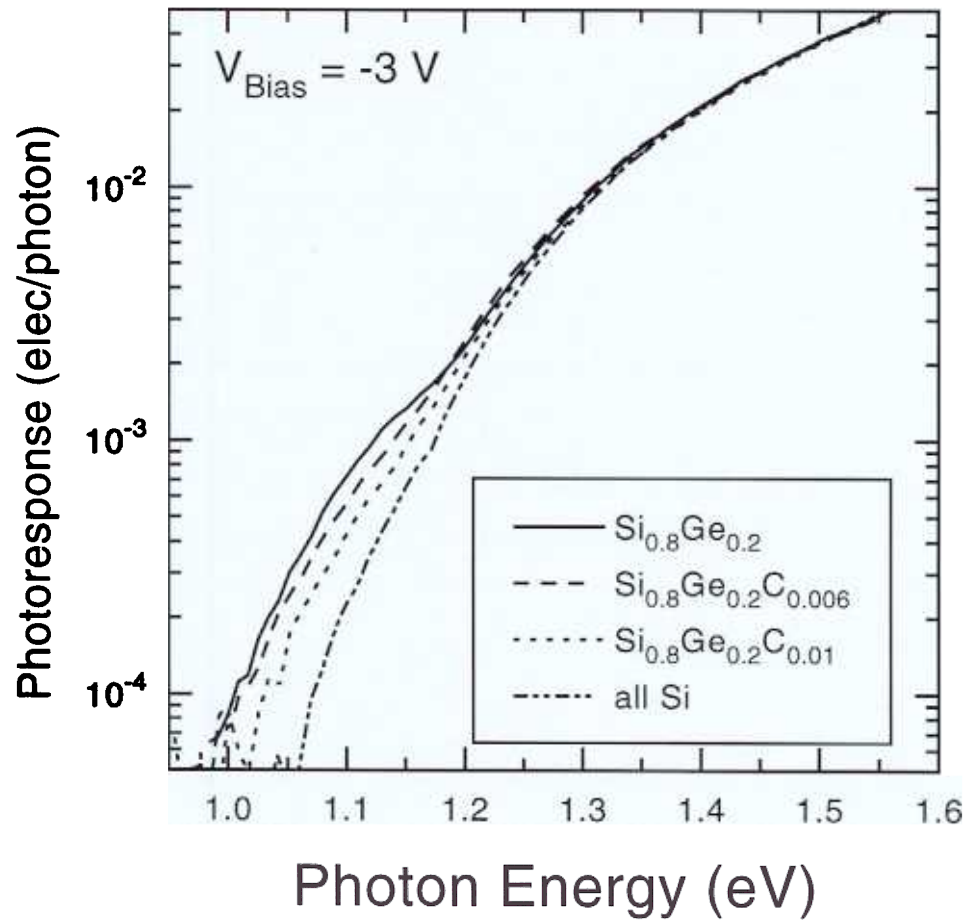


Figure 6.12: Photoresponse of  $\text{Si}_{1-x-y}\text{Ge}_x\text{C}_y$  *p-i-n* diodes.

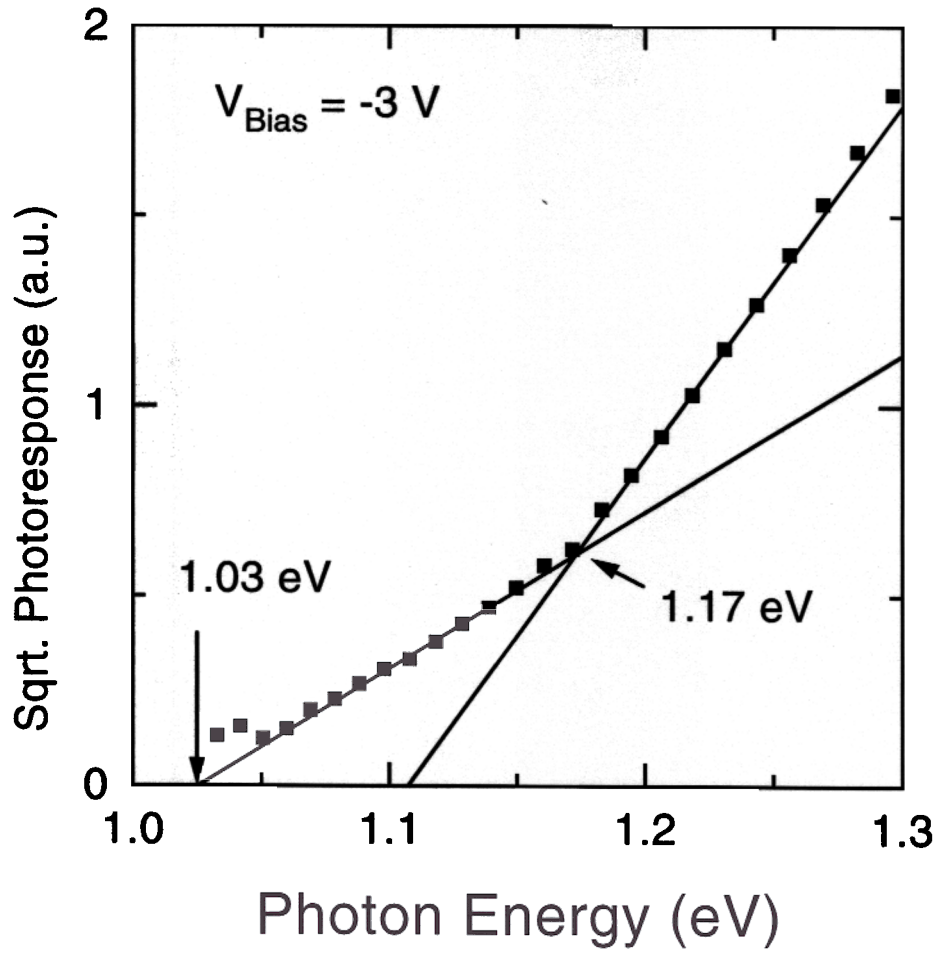


Figure 6.13: Photoresponse of all-Si diode.

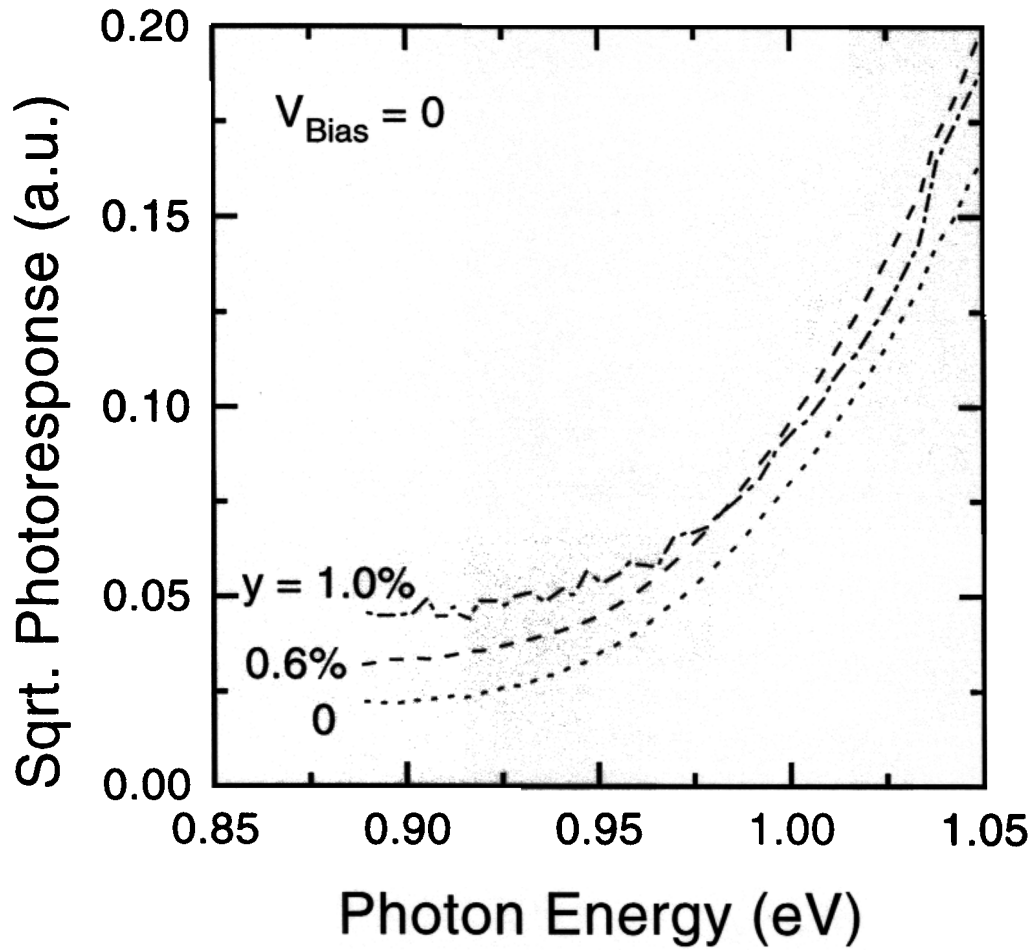


Figure 6.14: Photoresponse of  $\text{Si}_{1-x-y}\text{Ge}_x\text{C}_y$  *p-i-n* diodes.

## 6.5 Summary

In this chapter, we have described the optical and electrical characterization of pseudomorphic  $\text{Si}_{1-x-y}\text{Ge}_x\text{C}_y$  heterostructures. We have demonstrated the first defect-free band-edge PL from  $\text{Si}_{1-x-y}\text{Ge}_x\text{C}_y$ , and from this luminescence we have determined the band gap as a function of C concentration for both strained and relaxed  $\text{Si}_{1-x-y}\text{Ge}_x\text{C}_y$ . Our results indicate that, strain effects aside, the intrinsic effect of C is to reduce the band gap of  $\text{Si}_{1-x-y}\text{Ge}_x\text{C}_y$ . Furthermore, we have demonstrated that, for a given band gap,  $\text{Si}_{1-x-y}\text{Ge}_x\text{C}_y$  films have less strain and a greater critical thickness than do  $\text{Si}_{1-x}\text{Ge}_x$  films. This work clearly shows the potential technological importance of  $\text{Si}_{1-x-y}\text{Ge}_x\text{C}_y$  for strain-free heterostructures on Si.

For C concentrations less than 1.0%,  $\text{Si}_{1-x-y}\text{Ge}_x\text{C}_y$  *p-i-n* diodes showed no degradation in reverse bias leakage, but diodes with  $[C] \geq 1.0\%$  exhibited premature breakdown consistent with widely spaced point defects. Except at very low energies, all devices showed well behaved photoresponse spectra indicative of an indirect band gap of  $\sim 950$  meV. More precise band gap determination by photoresponse spectroscopy was not possible due to excess defect-related sub- $E_G$  absorption.

---

## Conclusion

### 7.1 Summary

This thesis has addressed two topics related to epitaxial Si-based heterostructures: the temperature dependence of luminescence in strained  $\text{Si}_{1-x}\text{Ge}_x/\text{Si}$  structures and the growth and characterization of strained  $\text{Si}_{1-x-y}\text{Ge}_x\text{C}_y$  films. We have experimentally identified the origin of the temperature dependence of photoluminescence intensity in strained  $\text{Si}_{1-x}\text{Ge}_x/\text{Si}$  quantum well structures and shown that passivation of the top Si surface can lead to greatly enhanced room temperature PL. This behavior was well modeled by coupling a commercial device simulator to a model for the luminescence intensity. Furthermore, we identified two causes for the observed difference in temperature dependence between photo- and electroluminescence. In the  $\text{Si}_{1-x-y}\text{Ge}_x\text{C}_y$  area, we developed an RTCVD process for the formation of high-quality pseudomorphic layers on Si (001) with up to 1.1% C. Photoluminescence from these layers was used to measure the band gap of both strained and relaxed  $\text{Si}_{1-x-y}\text{Ge}_x\text{C}_y$ . It was shown that the addition of C to strained  $\text{Si}_{1-x}\text{Ge}_x$  leads to an increased critical thickness for a given band gap.

### Future Work

One long held goal of those working with strained  $\text{Si}_{1-x}\text{Ge}_x$  has been the realization of a Si-based room temperature IR emitter. We have shown that the drop in PL intensity from cryogenic temperatures to room temperature is not an intrinsic property of  $\text{Si}_{1-x}\text{Ge}_x$ , but can be controlled by eliminating sources of non-radiative recombination. However, due to the indirect band gap of  $\text{Si}_{1-x}\text{Ge}_x$  alloys, the quantum efficiency of  $\text{Si}_{1-x}\text{Ge}_x$  quantum well LEDs will always be quite low. An emissive material with a higher radiative recombination probability is required to achieve an efficient IR source

Such materials may include Ge/Si short period superlattices and some organic materials.

$\text{Si}_{1-y}\text{C}_y$  and  $\text{Si}_{1-x-y}\text{Ge}_x\text{C}_y$  alloys are relatively new materials, with the first report of their formation in 1990. As such, there is a tremendous amount to be done. With such a range of possible growth techniques and process conditions, the huge parameter space has barely been explored. Finding the optimum technique for substitutional C incorporation should be a top priority. Understanding how large C doses affect the behavior of Si devices is very important if  $\text{Si}_{1-y}\text{C}_y$  and  $\text{Si}_{1-x-y}\text{Ge}_x\text{C}_y$  are to be incorporated into transistors and diodes. We know, for example, that C slows the diffusion of B and the formation of dislocations in Si by trapping Si self-interstitials[92]. Also, the available experimental evidence suggests that predicting the electronic band structure of  $\text{Si}_{1-y}\text{C}_y$  or  $\text{Si}_{1-x-y}\text{Ge}_x\text{C}_y$  cannot be done by interpolating between the constituent elements. Further experimental work is required to solidify our understanding of C's effect on band alignments as well as on band gaps and on transport properties such as lifetime and mobility. Finally, although they appear promising, it remains to be demonstrated that either  $\text{Si}_{1-y}\text{C}_y$  or  $\text{Si}_{1-x-y}\text{Ge}_x\text{C}_y$  is an enabling material which allows the realization of an otherwise unattainable, useful device.

## References

- [1] J. Matthews and A. Blakeslee, "Defects in epitaxial multilayers," *J. Cryst. Growth*, vol. 27, p. 118, 1974.
- [2] D. Houghton, C. Gibbings, C. Tuppen, M. Lyons, and M. Halliwell, "Equilibrium critical thickness for  $\text{Si}_{1-x}\text{Ge}_x$  strained layers on (100) Si," *Appl. Phys. Lett.*, vol. 56, p. 460, 1990.
- [3] J. Dismukes, L. Ekstrom, and R. Paff, "Lattice parameter and density in germanium-silicon alloys," *J. Phys. Chem.*, vol. 68, p. 3021, 1964.
- C. Van de Walle and R. Martin, "Theoretical calculations of heterojunction discontinuities in the Si/Ge system," *Phys. Rev.*, vol. B 34, p. 5621, 1986.
- [5] C. Van de Walle, "Band lineups and deformation potentials in the model-solid theory," *Phys. Rev.*, vol. B 39, p. 1871, 1989.
- R. Braunstein, A. Moore, and F. Herman, "Intrinsic optical absorption in germanium-silicon alloys," *Phys. Rev.*, vol. 109, p. 695, 1958.
- [7] D. Lang, R. People, J. Bean, and A. Sergent, "Measurement of the band gap of  $\text{Ge}_x\text{Si}_{1-x}/\text{Si}$  strained-layer heterostructures," *Appl. Phys. Lett.*, vol. 47, p. 1333, 1985.
- [8] D. Houghton, G. Aers, S. Yang, E. Wang, and N. Rowell, "Type I band alignment in  $\text{Si}_{1-x}\text{Ge}_x/\text{Si}(001)$  quantum wells: Photoluminescence under applied [110] and [100] uniaxial stress," *Phys. Rev. Lett.*, vol. 75, p. 866, 1995.

- [9] P. Kelires and J. Tersoff, "Equilibrium alloy properties by direct simulation: Oscillatory segregation at the Si-Ge(100)  $2\times 1$  surface," *Phys. Rev. Lett.*, vol. 63, p. 1164, 1989.
- J. Tersoff, "Stress-induced layer-by-layer growth of Ge on Si(100)," *Phys. Rev.*, vol. B 43, p. 9377, 1991
- J. Matthews, "Defects associated with the accommodation of misfit between crystals," *J. Vac. Sci. Technol.*, vol. 12, p. 126, 1975.
- [12] D. Houghton, D. Perovic, J.-M. Barbeau, and G. Weatherly, "Misfit strain in  $\text{Ge}_x\text{Si}_{1-x}$ /Si heterostructures: The structural stability of buried strained layers and strained-layer superlattices," *J. Appl. Phys.*, vol. 67, p. 1850, 1990.
- [13] R. People and J. Bean, "Calculation of critical layer thickness verses lattice mismatch for  $\text{Ge}_x\text{Si}_{1-x}$ /Si strained-layer heterostructures," *Appl. Phys. Lett.*, vol. 47, p. 322, 1985.
- [14] R. People and J. Bean, "Erratum: Calculation of critical layer thickness verses lattice mismatch for  $\text{Ge}_x\text{Si}_{1-x}$ /Si strained-layer heterostructures," *Appl. Phys. Lett.*, vol. 49, p. 229, 1986.
- [15] J. Weber and M. Alonso, "Near-band-gap photoluminescence of Si-Ge alloys," *Phys. Rev.*, vol. B 40, p. 5683, 1989.
- [16] J. Sturm, H. Manoharan, L. Lenchyshyn, M. Thewalt, N. Rowell, J.-P. Noël, and D. Houghton, "Well-resolved band-edge photoluminescence of excitons confined in strained  $\text{Si}_{1-x}\text{Ge}_x$  quantum wells," *Phys. Rev. Lett.*, vol. 66, p. 1362, 1991.
- [17] G. Bastard, *Wave Mechanics Applied to Semiconductor Heterostructures*, ch. 6. Halsted Press, 1988.

- [18] V. Venkataraman, *Physics and Applications of Si/Si<sub>1-x</sub>Ge<sub>x</sub> Modulation Doped Structures*. PhD thesis, Princeton University, 1994.
- [19] R. Sauer, J. Weber, J. Stolz, E. Weber, K.-H. Küsters, and H. Alexander, "Dislocation-related photoluminescence in Si," *Appl. Phys.*, vol. A 36, p. 1, 1985.
- [20] J.-P. Noël, N. Rowell, D. Houghton, and D. Perovic, "Intense photoluminescence between 1.3 and 1.8  $\mu\text{m}$  from strained Si<sub>1-x</sub>Ge<sub>x</sub> alloys," *Appl. Phys.Lett*, vol. 57, p. 1037, 1990.
- [21] J. Sturm, A. St. Amour, Y. Lacroix, and M. Thewalt, "Deep photoluminescence in Si/Si<sub>1-x</sub>Ge<sub>x</sub>/Si quantum wells created by ion implantation and annealing," *Appl. Phys.Lett*, vol. 64, p. 2291, 1994.
- [22] G. Mitchard and T. McGill, "Photoluminescence of Si-rich Si-Ge alloys," *Phys. Rev.*, vol. B 25, p. 5351, 1982.
- [23] X. Xiao, C. Liu, J. Sturm, L. Lenchyshyn, and M. Thewalt, "Photoluminescence from electron-hole plasmas confined in Si/Si<sub>1-x</sub>Ge<sub>x</sub>/Si quantum wells," *Appl. Phys.Lett*, vol. 60, p. 1720, 1992.
- [24] E. Cohen, M. Sturge, M. Olmstead, and R. Logan, "Electron-hole plasmas in photoexcited indirect-gap Al<sub>1-x</sub>Ga<sub>x</sub>As," *Phys. Rev.*, vol. B 22, p. 771, 1980.
- [25] X. Xiao, *Silicon-Germanium Alloys for Optoelectronic Applications*. PhD thesis, Princeton University, 1993.
- [26] H. Schlangenotto, H. Maeder, and W. Gerlach, "Temperature dependence of the radiative recombination coefficient in Si," *Phys. Stat. Sol.*, vol. A 21, p. 357, 1974.
- [27] W. Dumke, "Spontaneous radiative recombination in semiconductors," *Phys. Rev.*, vol. 105, p. 139, 1957.

- [28] V. Venkataraman. Private communication.
- [29] K. Terishima, M. Tajima, and T. Tatsumi, "Near-band-gap photoluminescence of  $\text{Si}_{1-x}\text{Ge}_x$  alloys grown on Si(100) by molecular beam epitaxy," *Appl. Phys. Lett.*, vol. 57, p. 1925, 1990.
- [30] D. Dutarte, G. Brémond, A. Souifi, and T. Benyattou, "Excitonic photoluminescence from Si-capped strained  $\text{Si}_{1-x}\text{Ge}_x$  layers," *Phys. Rev.*, vol. B 44, p. 11525, 1991.
- [31] J.-P. Noël, N. Rowell, D. Houghton, A. Wang, and D. Perovic, "Luminescence origins in molecular beam epitaxial  $\text{Si}_{1-x}\text{Ge}_x$ ," *Appl. Phys. Lett.*, vol. 61, p. 690, 1992.
- [32] S. Fukatsu, N. Usami, and Y. Shiraki, "Luminescence from strained  $\text{Si}_{1-x}\text{Ge}_x/\text{Si}$  quantum wells grown by Si molecular beam epitaxy," *Jpn. J. Appl. Phys.*, vol. 32, p. 1502, 1993.
- [33] M. Wachter, F. Schäffler, H.-J. Herzog, K. Thonke, and R. Sauer, "Photoluminescence of high-quality SiGe quantum wells grown by molecular beam epitaxy," *Appl. Phys. Lett.*, vol. 63, p. 376, 1993.
- [34] J. Sturm, A. St. Amour, Q. Mi, L. Lenchyshyn, and M. Thewalt, "High temperature (77-300 K) photo- and electroluminescence in Si/ $\text{Si}_{1-x}\text{Ge}_x$  heterostructures," *Jpn. J. Appl. Phys.*, vol. 33, p. 2329, 1994.
- [35] M. Gail, J. Brunner, U. Menczigar, Z. Zrenner, and G. Abstreiter, "Luminescence studies of MBE grown Si/SiGe quantum wells," *Mat. Res. Soc. Symp. Proc.*, vol. 298, p. 21, 1993.
- [36] N. Mott, *Metal-Insulator Transitions*. Taylor & Francis, 1990.

- [37] J. Shah, M. Combescot, and A. Dayem, "Investigation of exciton-plasma Mott transition in Si," *Phys. Rev. Lett.*, vol. 38, p. 1497, 1977.
- [38] P. Schwartz, *Oxygen Incorporation During Low-Temperature Chemical Vapor Deposition and Its Effects on the Electrical Properties of Epitaxial Si and Si<sub>1-x</sub>Ge<sub>x</sub> Films*. PhD thesis, Princeton University, 1992.
- [39] N. Ashcroft and N. Mermin, *Solid State Physics*, ch. 16. W.B. Saunders Co., 1976.
- [40] Technology Modeling Associates, Inc., Palo Alto, CA, *Medici: Two-Dimensional Device Simulation Program*. version 2.1.
- [41] A. St. Amour, J. Sturm, Y. Lacroix, and M. Thewalt, "Enhancement of high-temperature photoluminescence in strained Si<sub>1-x</sub>Ge<sub>x</sub>/Si heterostructures by surface passivation," *Appl. Phys. Lett.*, vol. 65, p. 3344, 1994.
- [42] A. St. Amour and J. Sturm, "Numerical simulation of the temperature dependence of photoluminescence in strained Si<sub>1-x</sub>Ge<sub>x</sub>/Si heterostructures," *J. Mater. Sci.: Mater. Elec.*, vol. 6, p. 350, 1995.
- [43] Q. Mi, X. Xiao, J. Sturm, L. Lenchyshyn, and M. Thewalt, "Room-temperature 1.3  $\mu\text{m}$  electroluminescence from strained Si<sub>1-x</sub>Ge<sub>x</sub>/Si quantum wells," *Appl. Phys. Lett.*, vol. 60, p. 3177, 1992.
- [44] D. Robbins, P. Calcott, and W. Leong, "Electroluminescence from a pseudomorphic SiGe alloy," *Appl. Phys. Lett.*, vol. 59, p. 1350, 1991.
- [45] J. Engvall, J. Olajos, H. Grimmeiss, H. Presting, H. Kibbel, and E. Kasper, "Electroluminescence at room temperature of a Si/Ge strained-layer superlattice," *Appl. Phys. Lett.*, vol. 63, p. 491, 1993.

- [46] J. Olajos, J. Engvall, H. Grimmeiss, U. Menczigar, M. Gail, G. Abstreiter, H. Kibbel, and H. Presting, "Photo- and electroluminescence in short-period Si/Ge superlattice structures," *Semi. Sci. Tech.*, vol. 9, p. 2011, 1994.
- [47] Q. Mi, X. Xiao, J. Sturm, L. Lenchyshyn, and M. Thewalt, "Room-temperature CW 1.3  $\mu\text{m}$  and 1.5  $\mu\text{m}$  electroluminescence from Si/SiGe quantum wells," *IEEE Res. Conf. Proc.*, p. VIB.7, 1992.
- [48] S. Iyer, K. Eberl, M. Goorsky, F. LeGoues, J. Tsang, and F. Cardone, "Synthesis of  $\text{Si}_{1-y}\text{C}_y$  alloys by molecular beam epitaxy," *Appl. Phys. Lett.*, vol. 60, p. 356, 1992.
- [49] W. Faschinger, S. Zerlauth, and G. Bauer, "Electrical properties of  $\text{Si}_{1-y}\text{C}_y$  alloys and modulation doped Si/ $\text{Si}_{1-y}\text{C}_y$ /Si structures," *Appl. Phys. Lett.*, vol. 67, p. 3933, 1995.
- [50] K. Brunner, K. Eberl, and W. Winter, "Near-band-edge photoluminescence from pseudomorphic  $\text{Si}_{1-y}\text{C}_y$ /Si quantum well structures," *Phys. Rev. Lett.*, vol. 76, p. 303, 1996.
- [51] K. Eberl, S. Iyer, S. Zollner, J. Tsang, and F. LeGoues, "Growth and strain compensation effects in the ternary  $\text{Si}_{1-x-y}\text{Ge}_x\text{C}_y$  alloy system," *Appl. Phys. Lett.*, vol. 60, p. 3033, 1992.
- [52] J. Regolini, F. Gisbert, G. Dolino, and P. Boucaud, "Growth and characterization of strain compensated  $\text{Si}_{1-x-y}\text{Ge}_x\text{C}_y$  epitaxial layers," *Mater. Lett.*, vol. 18, p. 57, 1993.
- [53] R. Series and K. Barraclough, "Control of carbon in Czochralski silicon crystals," *J. Cryst. Growth*, vol. 63, p. 219, 1983.

- [54] G. Davies and R. Newman, "Carbon in mono-crystalline silicon," in *Handbook on Semiconductors*, vol. 3b, pp. 1558–1635, New York: Elsevier, 1994.
- [55] A. Bean and R. Newman, "The solubility of carbon in pulled silicon crystals," *J. Phys. & Chem. Solids*, vol. 32, p. 1211, 1971
- [56] T. Nozaki, Y. Yatsurugi, and N. Akiyama, "Concentration and behavior of carbon in semiconductor silicon," *J. Electrochem. Soc.*, vol. 117, p. 1566, 1970.
- [57] W. Taylor, T. Tan, and U. Göele, "Carbon precipitation in silicon: Why is it so difficult?," *Appl. Phys. Lett.*, vol. 62, p. 3336, 1993.
- [58] F. Rollert, N. Stolwijk, and H. Mehrer *Mater. Sci. Forum*, vol. 38-41, p. 753, 1989.
- [59] R. Newman and J. Wakefield, "The diffusivity of carbon in silicon," *J. Phys. & Chem. Solids*, vol. 30, p. 230, 1961
- [60] A. Tipping and R. Newman, "An infrared study of the production, diffusion and complexing of interstitial boron in electron-irradiated silicon," *Semicond. Sci. & Technol.*, vol. 2, p. 389, 1987.
- [61] R. Newman, A. Oates, and F. Livingston, "Self-interstitials and thermal donor formation in silicon: new measurements and a model for the defects," *J. Phys.*, vol. C 16, p. L667, 1983.
- [62] S. Jain, H. Osten, B. Dietrich, and H. Rücker, "Growth and properties of strained  $\text{Si}_{1-x-y}\text{Ge}_x\text{C}_y$  layers," *Semicond. Sci. & Technol.*, vol. 10, p. 1289, 1995.
- [63] H. Rücker, M. Methfessel, E. Bugiel, and H. Osten, "Growth and properties of strained  $\text{Si}_{1-x-y}\text{Ge}_x\text{C}_y$  layers," *Phys. Rev. Lett.*, vol. 72, p. 3578, 1994.

## References

- [64] F. Johnson, "Lattice absorption bands in silicon," *Proc. Phys. Soc. London*, vol. 73, p. 265, 1959.
- [65] J. Baker, T. Tucker, N. Moyer, and R. Buschert, "Effect of carbon on the lattice parameter of silicon," *J. Appl. Phys.*, vol. 39, p. 4365, 1968.
- [66] B. Dietrich, H. Osten, H. Rucker, M. Methfessel, and P. Zaumseil, "Lattice distortion in a strain-compensated  $\text{Si}_{1-x-y}\text{Ge}_x\text{C}_y$  layer on silicon," *Phys. Rev.* vol. B 49, p. 49, 1994.
- [67] J. Mi, P. Warren, P. Letourneau, M. Judelewicz, M. Gailhanou, and M. Dutoit, "High quality  $\text{Si}_{1-x-y}\text{Ge}_x\text{C}_y$  epitaxial layers on (100) Si by rapid thermal chemical vapor deposition using methylsilane," *Appl. Phys. Lett.*, vol. 67, p. 259, 1995.
- [68] M. Todd, P. Matsunaga, J. Kouvetakis, D. Chandrasekhar, and D. Smith, "Growth of heteroepitaxial  $\text{Si}_{1-x-y}\text{Ge}_x\text{C}_y$  alloys on silicon using novel deposition chemistry," *Appl. Phys. Lett.*, vol. 67, p. 1247, 1995.
- [69] J. Strane, H. Stein, S. Lee, B. Doyle, S. Picraux, and J. Mayer, "Metastable SiGeC formation by solid phase epitaxy," *Appl. Phys. Lett.*, vol. 63, p. 2786, 1993.
- [70] S. Im, J. Washburn, R. Gronsky, N. Cheung, K. Yu, and J. Ager, "Optimization of Ge/C ratio for compensation of misfit strain in solid phase epitaxial growth of SiGe layers," *Appl. Phys. Lett.*, vol. 63, p. 2682, 1994.
- [71] H. Osten, E. Bugiel, and P. Zaumseil, "Growth of an inverse tetragonal distorted SiGe layer on Si(001) by adding small amounts of carbon," *Appl. Phys. Lett.*, vol. 64, p. 3440, 1994.
-

- [72] J. Posthill, R. Rudder, S. Hattangady, C. Fountain, and R. Markunas, "On the feasibility of growing dilute  $C_xSi_{1-x}$  epitaxial alloys," *Appl. Phys. Lett.*, vol. 56, p. 734, 1991.
- [73] A. St. Amour, C. Liu, J. Sturm, Y. Lacroix, and M. Thewalt, "Defect-free band-edge photoluminescence and band gap measurement of pseudomorphic  $Si_{1-x-y}Ge_xC_y$  alloy layers on Si (100)," *Appl. Phys. Lett.*, vol. 67, p. 3915, 1995.
- [74] W. Kissinger, M. Weidner, H. Osten, and M. Eichler, "Optical transitions in strained  $Si_{1-y}C_y$ -layers on Si(001)," *Appl. Phys. Lett.*, vol. 65, p. 3356, 1994.
- [75] C. Liu, A. St. Amour, J. Sturm, Y. Lacroix, and M. Thewalt, "Defect-free band-edge photoluminescence in  $Si_{1-x-y}Ge_xC_y$  strained layers grown by rapid thermal chemical vapor deposition," *Mat. Res. Soc. Sym. Proc.*, vol. 379, p. 441, 1995.
- [76] J. Sturm, P. Schwartz, E. Prinz, and H. Manoharan, "Growth of  $Si_{1-x}Ge_x$  by rapid thermal chemical vapor deposition and application to heterojunction bipolar transistors," *J. Vac. Sci. & Technol.*, vol. B 9, p. 2011, 1991.
- [77] C. Liu, A. St. Amour, J. Sturm, Y. Lacroix, M. Thewalt, C. Magee, and D. Eaglesham, "Growth and photoluminescence of high quality SiGeC random alloys on silicon substrates," *J. Appl. Phys.*, 1996. to be published.
- [78] B. Cullity, *Elements of X-ray Diffraction*, p. 99. Addison-Wesley, 1956
- [79] S. Bodnar and J. Regolini, "Growth of ternary alloy  $Si_{1-x-y}Ge_xC_y$  by rapid thermal chemical vapor deposition," *J. Vac. Sci. & Technol.*, vol. A 13, p. 2336, 1995.
- [80] P. Boucaud, C. Francis, F. Julien, J. Lourtioz, D. Bouchier, S. Bodnar, B. Lambert, and J. Regolini, "Band-edge and deep level photoluminescence of pseudomorphic  $Si_{1-x-y}Ge_xC_y$  alloys," *Appl. Phys. Lett.*, vol. 64, p. 875, 1994.

## References

- [81] L. Lanzerotti, A. St. Amour, C. Liu, J. Sturm, J. Watanabe, and N. Theodore, "Si/Si<sub>1-x-y</sub>Ge<sub>x</sub>C<sub>y</sub>/Si heterojunction bipolar transistors," *Elec. Dev. Lett.*, 1996 to be published.
- [82] J. Neugebauer and C. Van de Walle, "Electronic structure and phase stability of GaAs<sub>1-x</sub>N<sub>x</sub> alloys," *Phys. Rev.*, vol. B 48, p. 10568, 1995.
- [83] A. Demkov and F. Sankey, "Theoretical investigation of random Si-C alloys," *Phys. Rev.*, vol. B 48, p. 2207, 1993.
- [84] R. Soref, "Optical bandgap of the ternary semiconductor Si<sub>1-x-y</sub>Ge<sub>x</sub>C<sub>y</sub>," *J. Phys.*, vol. 70, p. 2470, 1991.
- [85] C. Chang, A. St. Amour, L. Lanzerotti, and J. Sturm, "Growth and electrical performance of heterojunction p<sup>+</sup> Si<sub>1-x-y</sub>Ge<sub>x</sub>C<sub>y</sub>/p<sup>-</sup> Si diodes," *Mat. Res. Soc. Sym. Proc.*, vol. 402, p. 437, 1995.
- [86] B. Roos, H. Richter, J. Osten, B. Tillack, J. Wollweber, and A. Wanner, "Mechanical properties of Si-Ge, Si-Ge-C and Si-Ge-B alloys," presented at the 1996 *Mater. Res. Soc. Spr. Mtg.*
- [87] W. Runyan and K. Bean, *Semiconductor Integrated Circuit Processing Technology*, ch. 11. New York: Addison-Wesley, 1990
- [88] G. Macfarlane and V. Roberts, "Infrared absorption of germanium near the lattice edge," *Phys. Rev.*, vol. 97, p. 1714, 1955.
- [89] J. Park, R. Karunasiri, and K. Wang, "Observation of large Stark shift in Ge<sub>x</sub>Si<sub>1-x</sub>/Si multiple quantum wells," *J. Vac. Sci. & Technol.*, vol. B 8, p. 217, 1990.

- [90] A. A. Chowdhury, M. M. Rashed, C. Mazier, S. Murtaza, and J. Cambell, "Room temperature observation of photocurrent dependence on applied bias in  $\text{Si}_{1-x}\text{Ge}_x/\text{Si}$  multiquantum wells," *J. Vac. Sci. & Technol.*, vol. B 11, p. 1685, 1993.
- [91] S. Murtaza, R. Mayer, M. Rashed, D. Kinosky, C. Mazier, S. Banerjee, A. Tasch, J. C. Campbell, J. C. Bean, and L. J. Peticolas, "Room temperature electroabsorption in a  $\text{Ge}_x\text{Si}_{1-x}$  PIN photodiode," *IEEE Trans. Elec. Dev.*, vol. 41, p. 2297, 1994.
- [92] T. Simpson, R. Goldberg, and I. Mitchell, "Suppression of dislocation formation in silicon by carbon implantation," *Appl. Phys. Lett.*, vol. 67, p. 2857, 1995.

## Medici Input Files

```

TITLE      Single Quantum Well for PL Simulation

COMMENT    Specify a "1D" Mesh Structure
MESH       OUT.FILE=qwm
X.MESH     WIDTH=0.050  N.SPACES=1

Y.MESH     N=1 L=-0.01
Y.MESH     N=3 L=0.0
Y.MESH     DEPTH=0.02  H1=0.0002
Y.MESH     DEPTH=0.007 H1=0.0002
Y.MESH     DEPTH=0.02 H1=0.0002 H2=0.002
Y.MESH     DEPTH=200 H1=0.02 H2=20

COMMENT    Use a SiGe layer (X.MOLE=0.35) with a graded mole fraction
+           for the transitions.
REGION    NUM=1  OXIDE Y.MIN=-0.01 Y.MAX=0
REGION    NUM=2  SILICON Y.MIN=0 Y.MAX=0.02
REGION    NUM=3  SIGE Y.MIN=0.02 Y.MAX=0.021 X.MOLE=0.0 X.END=0.35
REGION    NUM=3  SIGE Y.MIN=0.021 Y.MAX=0.026 X.MOLE=0.35
REGION    NUM=3  SIGE Y.MIN=0.026 Y.MAX=0.027 X.MOLE=0.35 X.END=0.0
REGION    NUM=2  SILICON Y.MIN=0.027

ELECTR    NUM=1  BOTTOM

PROFILE   P-TYPE N.PEAK=2e16 UNIFORM

MATERIAL  OXIDE
MATERIAL  SILICON TAUNO=1e-6 TAUP0=1e-6 AUGN=2.8e-31 AUGP=9.9e-32
MATERIAL  SIGE TAUNO=1e-6 TAUP0=1e-6 AUGN=2.8e-31 AUGP=9.9e-32

INTERFACE S.N=3e4 S.P=3e4

MODELS    SRH AUGER FERMI DIR INCOMPLE CCSMOB TEMP=250
  
```

## A. Medici Input Files

108

SYMBOL CARR=0 NEWTON  
METHOD ITLIMIT=200

SOLVE INIT

PHOTOGEN A3=4.2e21 A4=-1 Y.MIN=0

SYMBOL CARR=2 NEWTON

SOLVE

PLOT.1D VAL NEG X.ST=0 X.EN=0 Y.ST=0 Y.EN=200 MIN=-1.2 MAX=1.2  
+ TITLE="Band Diagram" OUT.FILE=val DEVICE=POSTSCRIPT  
+ PLOT.OUT=band.ps

PLOT.1D CON NEG X.ST=0 X.EN=0 Y.ST=0 Y.EN=200 MIN=-1.2 MAX=1.2  
+ OUT.FILE=con UNCH

PLOT.1D QFP NEG X.ST=0 X.EN=0 Y.ST=0 Y.EN=200 MIN=-1.2 MAX=1.2  
+ OUT.FILE=qfp UNCH

PLOT.1D QFN NEG X.ST=0 X.EN=0 Y.ST=0 Y.EN=200 MIN=-1.2 MAX=1.2  
+ OUT.FILE=qfn UNCH

PLOT.1D ELEC X.ST=0 X.EN=0 Y.ST=0 Y.EN=200 Y.LOG MAX=1e20 MIN=1e10  
+ OUT.FILE=elec

+ DEVICE=POSTSCRIPT PLOT.OUT=eh.ps

PLOT.1D HOLES X.ST=0 X.EN=0 Y.ST=0 Y.EN=200 Y.LOG OUT.FILE=hole  
+ UNCH

PLOT.1D PHOTOGEN X.ST=0 X.EN=0 Y.ST=0 Y.EN=10 Y.LOG OUT.FILE=photo  
+ DEVICE=POSTSCRIPT PLOT.OUT=photo.ps

PLOT.1D RECOMB X.ST=0 X.EN=0 Y.ST=0 Y.EN=200 OUT.FILE=recomb  
+ DEVICE=POSTSCRIPT PLOT.OUT=recomb.ps Y.LOG

```

TITLE      Single Quantum Well p-i-n Diode for EL Simulation

COMMENT    Specify a "1D" Mesh Structure
MESH      OUT.FILE=qwm
X.MESH    WIDTH=1  N.SPACES=1

Y.MESH    DEPTH=0.1  H1=0.02
Y.MESH    DEPTH=0.13 H1=0.01 H2=0.0002
Y.MESH    DEPTH=0.007 H1=0.0002
Y.MESH    DEPTH=0.03 H1=0.001
Y.MESH    DEPTH=0.4  H1=0.001 H2=0.02
Y.MESH    DEPTH=2.0  H1=0.02
$ Y.MESH  DEPTH=200 H1=0.02 H2=5

COMMENT    Use a SiGe layer (X.MOLE=0.35) with a graded mole fraction
+          for the transitions.
REGION    NUM=1  SILICON Y.MIN=0 Y.MAX=0.1
REGION    NUM=2  SILICON Y.MIN=0.1 Y.MAX=0.23
REGION    NUM=3  SIGE Y.MIN=0.23 Y.MAX=0.231 X.MOLE=0.0 X.END=0.35
REGION    NUM=3  SIGE Y.MIN=0.231 Y.MAX=0.236 X.MOLE=0.35
REGION    NUM=3  SIGE Y.MIN=0.236 Y.MAX=0.237 X.MOLE=0.35 X.END=0.0
REGION    NUM=2  SILICON Y.MIN=0.237 Y.MAX=0.267
REGION    NUM=2  SILICON Y.MIN=0.267 Y.MAX=0.667
REGION    NUM=4  SILICON Y.MIN=0.667 Y.MAX=2.667
$ REGION    NUM=2  SILICON Y.MIN=2.667

ELECTR    NUM=1  BOTTOM
ELECTR    NUM=2  TOP

PROFILE   P-TYPE N.PEAK=1e20 UNIFORM REGION=1
PROFILE   N-TYPE N.PEAK=1e16 UNIFORM REGION=2
PROFILE   N-TYPE N.PEAK=1e16 UNIFORM REGION=3
PROFILE   N-TYPE N.PEAK=1e20 UNIFORM REGION=4

CONTACT NUM=1 VOLTAGE
$ CONTACT NUM=2 CURRENT NEUTRAL

MATERIAL SILICON TAUNO=1e-6 TAUP0=1e-6 AUGN=2.8e-31 AUGP=9.9e-32
MATERIAL SIGE TAUNO=1e-6 TAUP0=1e-6 AUGN=2.8e-31 AUGP=9.9e-32

MODELS    SRH AUGER FERMIDIR INCOMPLE CCSMOB TEMP=250
SYMBOL    CARR=0 NEWTON
METHOD    ITLIMIT=200

SOLVE I2=0 V1=0
CONTACT NUM=2 CURRENT NEUTRAL
SYMBOL CARR=2 NEWTON

```

SOLVE I2=0 V1=0

SOLVE I2=0.67E-9 V1=0

```
PLOT.1D VAL NEG X.ST=0 X.EN=0 Y.ST=0 Y.EN=2.667 MIN=-1.2 MAX=1.2
+ TITLE="Band diagram" OUT.FILE=val DEVICE=POSTSCRIPT
+ PLOT.OUT=band.ps
PLOT.1D CON NEG X.ST=0 X.EN=0 Y.ST=0 Y.EN=2.667 MIN=-1.2 MAX=1.2
+ OUT.FILE=con UNCH
PLOT.1D QFP NEG X.ST=0 X.EN=0 Y.ST=0 Y.EN=2.667 MIN=-1.2 MAX=1.2
+ OUT.FILE=qfp UNCH
PLOT.1D QFN NEG X.ST=0 X.EN=0 Y.ST=0 Y.EN=2.667 MIN=-1.2 MAX=1.2
+ OUT.FILE=qfn UNCH

PLOT.1D ELEC X.ST=0 X.EN=0 Y.ST=0 Y.EN=2.667 Y.LOG
+ OUT.FILE=elec
+ DEVICE=POSTSCRIPT PLOT.OUT=eh.ps
PLOT.1D HOLES X.ST=0 X.EN=0 Y.ST=0 Y.EN=2.667 Y.LOG OUT.FILE=hole
+ UNCH

PLOT.1D J.ELECTR X.ST=0 X.EN=0 Y.ST=0 Y.EN=2.667 OUT.FILE=ie
+ DEVICE=POSTSCRIPT PLOT.OUT=i.ps
PLOT.1D J.HOLE X.ST=0 X.EN=0 Y.ST=0 Y.EN=2.667 OUT.FILE=ih UNCH

PLOT.1D RECOMB X.ST=0 X.EN=0 Y.ST=0 Y.EN=2.667 OUT.FILE=recomb
+ DEVICE=POSTSCRIPT PLOT.OUT=recomb.ps Y.LOG
```

**Growth Sequences**

B.1  $\text{Si}_{1-x-y}\text{Ge}_x\text{C}_y$  PL Sample #1740

Sequencer Table #0

Step #	Action	Comment
0	CONTROL ON&	Turn on Control
1	SCAN ON(0.3) and	Scan simultaneously
2	SET(SP7,0)&	Override power to zero
3	SET(SP4,0)&	Turn off PID control
4		
5	SET(D00,1)&	N2 off
6	SET(D01,0)&	H2 off
7	SET(D02,1)&	GeH4 select on
8	SET(D03,0)&	SiH4 off
9	SET(D04,0)&	B2H6 off
10	SET(D05,0)&	PH3 off
11	SET(D06,1)&	X on
12	SET(D07,1)&	DCS on
13	SET(D08,0)	SiCH6 off
14	SET(D09,0)&	GeH4 inject off
15	SET(D010,0)&	SiH4 off
16	SET(D011,0)&	B2H6 off
17	SET(D012,0)&	PH3 off
18	SET(D013,0)	Source off
19	SET(A00,0.617)&	H2 flow = 3 slpm
20	SET(D015,1)	Vacuum on
21	SET(D01,1)&	H2 on
22	SET(A01,0.212)&	GeH4 flow = 100 sccm
23	SET(A02,0.01)&	SiH4
24	SET(A03,0.01)&	B2H6 high
25	SET(A04,0.01)&	PH3 high
26	SET(A05,0.01)&	PH3 low
27	SET(A06,0.537)&	DCS flow = 26 sccm
28	SET(A07,0.063)	SiCH6 flow = 5 sccm
29	SET(A08,0.0)	Pressure = 0
30	SEQUENCER ON(0.3,1,0)	Start Sequencer #1
31		

## B. Growth Sequences

113

Sequencer Table #1

Step #	Action	Comment
0		
1	SET(SP2,0.0)&	Reset loop control
2	SEQUENCER ON(0.3,6,0)	Call cleaning sequence
3	WAITUNTIL(SP2>0.5)	Cleaning sequence
4	SET(SP2,0.0)&	Reset loop control
5		
6	SEQUENCER ON(0.3,5,0)	Call buffer sequence
7	WAITUNTIL(SP2>0.5)	Buffer sequence
8	SET(SP2,0.0)&	Reset loop control
9		
10		
11		
12	SEQUENCER ON(0.3,4,0)	Call SiGeC sequence
13	WAITUNTIL(SP2>0.5)	SiGeC sequence
14	SET(SP2,0.0)&	Reset loop control
15		
16	SET(SP4,0.0)	Feedback off
17		
18		
19	RAMP(SP7,-0.4,0.0)	Lamps down to 0
20		
21		
22		
23		
24		
25		
26	SEQUENCER ON(0.3,7,0)	Call reload sequence
27		
28		
29		
30		
31		

## B. Growth Sequences

114

Sequencer Table #4

Step #	Action	Comment
0	SET(SP5,1.92)	Set T = 575C
1	SET(SP4,1.0)	Closed-loop
2	SET(D013,0)	DCS inject off
3	SET(D08,1)	Select SiCH6
4		
5		
6	WAITUNTIL(AI24>0.5)	GO when stable
7	SET(D013,1)&	Inject DCS and SiCH6
8	SET(D09,1)	Inject GeH4
9	WAIT(600)	SiGeC layer
10	SET(D09,0)	GeH4 inject off
11		Close SiCH6 manual valve
12	WAIT(30)	
13	SET(D02,0)	GeH4 select off
14		
15		
16	SET(SP5,3.31)	T = 675C
17	WAIT(600)	Si cap
18	SET(D013,0)	DCS inject off
19	SET(D07,0)	DCS select off
20	SET(SP2,1.0)	Set loop control
21	END	
22		
23		
24		
25		
26		
27		
28		
29		
30		
31		

## B. Growth Sequences

115

Sequencer Table #5

Step #	Action	Comment
0	WAITUNTIL(AI29<10)	Pumping out
1	WAITUNTIL(AI24>0.5)	GO for buffer
2	SET(AO11,1.0)&	Low pressure select
3	WAITUNTIL(AI28<5.5)	Pressure stabilizing
4	SET(AO8,0.60)&	Set P=6torr
5	WAITUNTIL(AI28>5.5)	Pressure stabilizing
6		
7		
8		
9	SET(DO13,1)	Inject DCS
10	WAIT(360)	Buffer I
11	SET(DO13,0)&	DCS inject off
12		
13		
14		
15	RAMP(SP7,-0.4,0.0)	Lamps off
16		
17		
18	WAITUNTIL(AI24>0.5)	GO for cold values
19	SET(SP3,1)	Get cold values
20	WAIT(1)	
21	SET(SP3,0)	Latch cold values
22		
23	RAMP(SP7,0.4,0.2)	Reheat wafer
24	WAIT(60)	Clean
25		
26		
27	SET(DO13,1)	Inject DCS
28	WAIT(60)	Buffer II
29	RAMP(SP7,-0.4,0.14)	Lamps down to 14%
30	WAIT(60)	Si at 14%
31	SET(SP2,1.0)	Set loop control

Sequencer Table #6

Step #	Action	Comment
0	WAITUNTIL(AI24>0.5)	GO for clean
1	SET(A011,0)&	High pressure select
2	SET(A08,0.250)&	P=250torr
3	SET(A00,0.817)&	H2 flow=4slpm
4	WAITUNTIL(AI29>250)	Pressure stabilizing
5		
6		
7		
8		
9		
10		
11		
12		
13		
14		
15		
16		
17		
18		
19		
20		
21		
22		
23		
24		
25		
26		
27	RAMP(SP7,0.4.0.274)	Lamps to 1000C
28	WAIT(120)	Clean
29	SET(A08,0.0)&	Pump out
30	SET(A00,0.617)&	H2 flow=3slpm
31	SET(SP2,1.0)	Set loop control

## B. Growth Sequences

117

Sequencer Table #7

Step #	Action	Comment
0	SET(SP7,0)	Lamps off
1	SET(D013,0)&	DCS inject off
2	SET(D012,0)&	PH3 off
3	SET(D011,0)&	B2H6 off
4	SET(D010,0)&	SiH4 off
5	SET(D09,0)&	GeH4 off
6	SET(D07,0)&	DCS select off
7	SET(D05,0)&	PH3 off
8	SET(D04,0)&	B2H6 off
9	SET(D03,0)	SiH4 off
10	SET(D02,0)&	GeH4 off
11	SET(D01,0)&	H2 off
12	SET(A08,0.0)&	Pump out
13	SET(A07,0.0)&	B2H6 low
14	SET(A06,0.0)&	DCS
15	SET(A05,0.0)&	PH3 low
16	SET(A04,0.0)&	PH3 high
17	SET(A03,0.0)&	B2H6 high
18	SET(A02,0.0)&	SiH4
19	SET(A01,0.0)&	GeH4
20	SET(A00,0.00)	H2
21	WAITUNTIL(AI28<0.5)	Pump out
22	SET(D015,0)	Vacuum off
23		
24	SEQUNCER OFF(0)	Sequencer 0 off
25	SEQUNCER OFF(1)	Sequencer 1 off
26	SEQUNCER OFF(2)	Sequencer 2 off
27	SEQUNCER OFF(3)	Sequencer 3 off
28	SEQUNCER OFF(4)	Sequencer 4 off
29	SEQUNCER OFF(5)	Sequencer 5 off
30	SEQUNCER OFF(6)	Sequencer 6 off
31	SEQUNCER OFF(7)	Sequencer 7 off

B.2  $\text{Si}_{1-x-y}\text{Ge}_x\text{C}_y$  *p-i-n* Sample #1876

Sequencer Table #0

Step #	Action	Comment
0	CONTROL ON&	Turn on Control
1	SCAN ON(0.3)	and Scan simultaneously
2	SET(SP7,0)&	Override power to zero
3	SET(SP4,0)&	Turn off PID control
4		
5	SET(D00,1)&	N2 off
6	SET(D01,0)&	H2 off
7	SET(D02,1)&	GeH4 select on
8	SET(D03,0)&	SiH4 off
9	SET(D04,1)&	B2H6 on
10	SET(D05,1)&	PH3 on
11	SET(D06,1)&	X on
12	SET(D07,1)&	DCS on
13	SET(D08,1)	SiCH6 on, man valve closed
14	SET(D09,0)&	GeH4 inject off
15	SET(D010,0)&	SiH4 off
16	SET(D011,0)&	B2H6 off
17	SET(D012,0)&	PH3 off
18	SET(D013,0)	Source off
19	SET(A00,0.617)&	H2 flow = 3 slpm
20	SET(D015,1)	Vacuum on
21	SET(D01,1)&	H2 on
22	SET(A01,0.212)&	GeH4 flow = 100 sccm
23	SET(A02,0.01)&	SiH4
24	SET(A03,0.353)&	B2H6 flow=170 sccm
25	SET(A04,0.616)&	PH3 flow=300 sccm
26	SET(A05,0.01)&	PH3 low
27	SET(A06,0.537)&	DCS flow = 26 sccm
28	SET(A07,0.063)	SiCH6 flow = 5 sccm
29	SET(A08,0.0)	Pressure = 0
30	SEQUENCER ON(0.3,1,0)	Start Sequencer #1
31		

## B. Growth Sequences

119

Sequencer Table #1

Step #	Action	Comment
0		
1	SET(SP2,0.0)&	Reset loop control
2	SEQUENCER ON(0.3,6,0)	Call cleaning sequence
3	WAITUNTIL(SP2>0.5)	Cleaning sequence
4	SET(SP2,0.0)&	Reset loop control
5	RAMP(SP7,-0.4,0.155)	Lamps down to 15.5%
6	WAIT(60)	
7	SEQUENCER ON(0.3,5,0)	Call buffer sequence
8	WAITUNTIL(SP2>0.5)	Buffer sequence
9	SET(SP2,0.0)&	Reset loop control
10		
11		
12	SEQUENCER ON(0.3,4,0)	Call SiGeC sequence
13	WAITUNTIL(SP2>0.5)	SiGeC sequence
14	SET(SP2,0.0)&	Reset loop control
15		
16	SET(SP4,0.0)	Feedback off
17		
18		
19	RAMP(SP7,-0.4,0.0)	Lamps down to 0
20		
21		
22		
23		
24		
25		
26	SEQUENCER ON(0.3,7,0)	Call reload sequence
27		
28		
29		
30		
31		

## B. Growth Sequences

120

Sequencer Table #4

Step #	Action	Comment
0	SET(SP5,3.579)	Set T = 700C
1	SET(SP4,1.0)	Closed-loop
2	WAIT(600)	Undoped Si
3	SET(SP5,2.984)	T = 625C
4	SET(D013,0)	DCS inject off
5		SiCH6 already selected
6	WAIT(15)	Open manual SiCH6 inject
7	SET(D013,1)&	Inject DCS and SiCH6
8	SET(D09,1)	Inject GeH4
9	WAIT(420)	SiGeC layer
10	SET(D09,0)	GeH4 inject off
11		Close SiCH6 manual valve
12	WAIT(30)	
13	SET(D02,0)	GeH4 select off
14	SET(SP5,3.579)	T = 700C
15	WAIT(600)	Undoped Si
16	SET(D012,1)	Inject PH3
17	WAIT(750)	p-type Si
18	SET(D013,0)&	DCS inject off
19	SET(D012,0)	PH3 inject off
20	SET(SP2,1.0)	Set loop control
21	END	
22		
23		
24		
25		
26		
27		
28		
29		
30		
31		

## B. Growth Sequences

121

Sequencer Table #5

Step #	Action	Comment
0	WAITUNTIL(AI29<10)	Pumping out
1	WAITUNTIL(AI24>0.5)	GO for buffer
2	SET(A011,1.0)&	Low pressure select
3	WAITUNTIL(AI28<5.5)	Pressure stabilizing
4	SET(A08,0.60)&	Set P=6torr
5	WAITUNTIL(AI28>5.5)	Pressure stabilizing
6		
7		
8	SET(D013,1)&	Inject DCS
9	SET(D011,1)	Inject B2H6
10	WAIT(300)	Buffer I
11	SET(D013,0)&	DCS inject off
12	SET(D011,0)	B2H6 inject off
13		
14		
15	RAMP(SP7,-0.4,0.0)	Lamps off
16		
17		
18	WAITUNTIL(AI24>0.5)	GO for cold values
19	SET(SP3,1)	Get cold values
20	WAIT(1)	
21	SET(SP3,0)	Latch cold values
22		
23	RAMP(SP7,0.4,0.274)	Reheat wafer
24	WAIT(60)	Clean
25		
26	SET(D011,1)&	Inject B2H6
27	SET(D013,1)	Inject DCS
28	WAIT(60)	Buffer II
29	SET(D011,0)	B2H6 inject off
30	SET(D04,0)	B2H6 select off
31	SET(SP2,1.0)	Set loop control

## B. Growth Sequences

122

Sequencer Table #6

Step #	Action	Comment
0	WAITUNTIL(AI24>0.5)	GO for clean
1	SET(A011,0)&	High pressure select
2	SET(A08,0.250)&	P=250torr
3	SET(A00,0.817)&	H2 flow=4slpm
4	WAITUNTIL(AI29>250)	Pressure stabilizing
5		
6		
7		
8		
9		
10		
11		
12		
13		
14		
15		
16		
17		
18		
19		
20		
21		
22		
23		
24		
25		
26		
27	RAMP(SP7,0.4.0.274)	Lamps to 1000C
28	WAIT(120)	Clean
29	SET(A08,0.0)&	Pump out
30	SET(A00,0.617)&	H2 flow=3slpm
31	SET(SP2,1.0)	Set loop control

## B. Growth Sequences

123

Sequencer Table #7

Step #	Action	Comment
0	SET(SP7,0)	Lamps off
1	SET(D013,0)&	DCS inject off
2	SET(D012,0)&	PH3 off
3	SET(D011,0)&	B2H6 off
4	SET(D010,0)&	SiH4 off
5	SET(D09,0)&	GeH4 off
6	SET(D07,0)&	DCS select off
7	SET(D05,0)&	PH3 off
8	SET(D04,0)&	B2H6 off
9	SET(D03,0)	SiH4 off
10	SET(D02,0)&	GeH4 off
11	SET(D01,0)&	H2 off
12	SET(A08,0.0)&	Pump out
13	SET(A07,0.0)&	B2H6 low
14	SET(A06,0.0)&	DCS
15	SET(A05,0.0)&	PH3 low
16	SET(A04,0.0)&	PH3 high
17	SET(A03,0.0)&	B2H6 high
18	SET(A02,0.0)&	SiH4
19	SET(A01,0.0)&	GeH4
20	SET(A00,0.00)	H2
21	WAITUNTIL(AI28<0.5)	Pump out
22	SET(D015,0)	Vacuum off
23		
24	SEQUNCER OFF(0)	Sequencer 0 off
25	SEQUNCER OFF(1)	Sequencer 1 off
26	SEQUNCER OFF(2)	Sequencer 2 off
27	SEQUNCER OFF(3)	Sequencer 3 off
28	SEQUNCER OFF(4)	Sequencer 4 off
29	SEQUNCER OFF(5)	Sequencer 5 off
30	SEQUNCER OFF(6)	Sequencer 6 off
31	SEQUNCER OFF(7)	Sequencer 7 off

### Publications and Presentations Resulting from this Thesis

#### Publications

1. A. St. Amour, L.D. Lanzerotti, C.L. Chang, and J.C. Sturm, "Optical and electrical properties of  $\text{Si}_{1-x-y}\text{Ge}_x\text{C}_y$  thin films and devices," to be published in *Thin Solid Films* (1996).
2. C.W. Liu, A. St. Amour, J.C. Sturm, Y.R.J. Lacroix, M.L.W. Thewalt, C.W. Evans, and D. Eaglesham, "Growth and photoluminescence of high quality SiGeC random alloys on silicon substrates," to be published in *J. Appl. Phys.* (1996).
3. L.D. Lanzerotti, A. St. Amour, C.W. Liu, J.C. Sturm, J.K. Watanabe, and N.D. Theodore, "Si/Si $_{1-x-y}$ Ge $_x$ C $_y$ /Si heterojunction bipolar transistors," to be published in *Elec. Dev. Lett.* (1996).
4. C.L. Chang, A. St. Amour, L.D. Lanzerotti, and J.C. Sturm, "Growth and electrical performance of heterojunction p $^+$ -Si $_{1-x-y}$ Ge $_x$ C $_y$ /p $^-$ -Si diodes," *Mat. Res. Soc. Symp. Proc.* 402 (1996) 437.

### C. Publications and Presentations Resulting from this Thesis

5. A. St. Amour, C.W. Liu, J.C. Sturm, Y. Lacroix, and M.L.W. Thewalt, "Defect-free band-edge photoluminescence and band gap measurement in pseudomorphic  $\text{Si}_{1-x-y}\text{Ge}_x\text{C}_y$  alloy layers on Si (100)," *Appl. Phys. Lett.* **67** (1995) 3915.
  6. A. St. Amour and J.C. Sturm, "Numerical simulation of the temperature dependence of band-edge photoluminescence and electroluminescence in strained- $\text{Si}_{1-x}\text{Ge}_x/\text{Si}$  heterostructures," *IEDM Tech. Digest* (1995) 769.
  7. A. St. Amour and J.C. Sturm, "Numerical simulation of the temperature dependence of photoluminescence in strained- $\text{Si}_{1-x}\text{Ge}_x/\text{Si}$  heterostructures," *J. Sci.: Mat. Elec.* **6** (1995) 350.
  8. J.C. Sturm, A. St. Amour, Y. Lacroix, and M.L.W. Thewalt, "Luminescence in  $\text{Si}_{1-x}\text{Ge}_x$  heterostructures," *Mat. Res. Soc. Symp. Proc.* **379** (1995) 387.
  9. C.W. Liu, A. St. Amour, J.C. Sturm, Y. Lacroix, and M.L.W. Thewalt, "Defect-free band-edge photoluminescence in  $\text{Si}_{1-x-y}\text{Ge}_x\text{C}_y$  strained layers grown by rapid thermal chemical vapor deposition," *Mat. Res. Soc. Symp. Proc.* **379** (1995) 441.
  10. A. St. Amour, J.C. Sturm, Y. Lacroix, and M.L.W. Thewalt, "Enhancement of high-temperature photoluminescence in strained- $\text{Si}_{1-x}\text{Ge}_x/\text{Si}$  heterostructures by surface passivation," *Appl. Phys. Lett.* **65** (1994) 3344
  11. L.D. Lanzerotti, A. St. Amour, and J.C. Sturm, "Si/ $\text{Si}_{1-x-y}\text{Ge}_x\text{C}_y$ /Si heterojunction bipolar transistors," *IEDM Tech. Digest* (1994) 930.
  12. J.C. Sturm, A. St. Amour, Q. Mi, L.C. Lenchyshyn, and M.L.W. Thewalt, "High-temperature (77-300 K) photo- and electroluminescence in  $\text{Si}/\text{Si}_{1-x}\text{Ge}_x$  heterostructures," *Jpn. J. Appl. Phys.* **33** (1994) 2329.
-

13. J.C. Sturm, A. St. Amour, Y. Lacroix, and M.L.W. Thewalt, "Deep photoluminescence in Si/Si<sub>1-x</sub>Ge<sub>x</sub>/Si quantum wells created by ion implantation and annealing," *Appl. Phys. Lett.* **64** (1994) 2291.
14. A. St. Amour and J.C. Sturm, "Deposition of monolayer-scale Ge/Si heterostructures by rapid thermal chemical vapor deposition," *Mat. Res. Soc. Symp. Proc.* **342** (1994) 31.
15. J.C. Sturm, X. Xiao, Q. Mi, C.W. Liu, A. St. Amour, Z. Matutinovic-Krstelj, L.C. Lenchyshyn, and M.L.W. Thewalt, "Photoluminescence and electroluminescence processes in Si/Si<sub>1-x</sub>Ge<sub>x</sub>/Si heterostructures grown by chemical vapor deposition," *Mat. Sci. Eng.* **B21** (1993) 307.
16. (invited) J.C. Sturm, X. Xiao, Q. Mi, A. St. Amour, L.C. Lenchyshyn, and M.L.W. Thewalt, "Opto-electronic applications of Si<sub>1-x</sub>Ge<sub>x</sub> heterostructures," *SSDM Tech. Digest* (1993) 198.

### Conference Presentations

1. (invited) A. St. Amour, L.D. Lanzerotti, C.L. Chang, J.C. Sturm, Y. Lacroix, and M.L.W. Thewalt, "Optical and electrical properties of Si<sub>1-x-y</sub>Ge<sub>x</sub>C<sub>y</sub> thin films and devices," *European Mat. Res. Soc. Spr. Mtg.*, Strasbourg, France (1996).
2. (invited) J.C. Sturm and A. St. Amour, "Low temperature chemical vapor deposition of column-IV heterostructures," *Electrochem. Soc. Mtg.*, Los Angeles, CA (1996).
3. A. St. Amour and J.C. Sturm, "Pseudomorphic Si<sub>1-x-y</sub>Ge<sub>x</sub>C<sub>y</sub> p-i-n diodes with low leakage current," *Mat. Res. Soc. Spr. Mtg.*, San Francisco, CA (1996).

4. (invited) J.C. Sturm, A. St. Amour, L.D. Lanzerotti, C.L. Chang, Y. Lacroix, and M.L.W. Thewalt, "Optical and electrical properties of  $\text{Si}_{1-x-y}\text{Ge}_x\text{C}_y$  structures grown by RTCVD," *Mat. Res. Soc. Spr. Mtg.*, San Francisco, CA (1996).
5. R.A. Donaton, K. Maex, A. Vantomme, A. St. Amour, and J.C. Sturm, "Comparison of Co silicidation on  $\text{Si}_{1-x}\text{Ge}_x$  and  $\text{Si}_{1-x-y}\text{Ge}_x\text{C}_y$  alloys," *Mat. Res. Soc. Spr. Mtg.*, San Francisco, CA (1996).
6. A. St. Amour and J.C. Sturm, "Numerical simulation of the temperature dependence of band-edge photoluminescence and electroluminescence in strained- $\text{Si}_{1-x}\text{Ge}_x/\text{Si}$  heterostructures," *Int. Elec. Dev. Mtg.*, Washington, DC (1995).
7. C.L. Chang, A. St. Amour, L.D. Lanzerotti, and J.C. Sturm, "Growth and electrical performance of heterojunction  $\text{p}^+-\text{Si}_{1-x-y}\text{Ge}_x\text{C}_y/\text{p}^--\text{Si}$  diodes," *Mat. Res. Soc. Fall Mtg.*, Boston, MA (1995).
8. A. St. Amour and J.C. Sturm, "High-quality pseudomorphic  $\text{Si}_{1-x-y}\text{Ge}_x\text{C}_y$  alloys grown on Si (100) by rapid thermal chemical vapor deposition," NATO ASI: *Advances in Rapid Thermal and Integrated Processing*, Maratea, Italy (1995).
9. A. St. Amour, J.C. Sturm, K. Brunner, J. Weber, Y. Lacroix, and M.L.W. Thewalt, "Band-edge photoluminescence in pseudomorphically strained  $\text{Si}_{1-x-y}\text{Ge}_x\text{C}_y$  layers on Si (100) substrates," *Elec. Mat. Conf.*, Charlottesville, VA (1995).
10. (invited) J.C. Sturm, A. St. Amour, Y. Lacroix, and M.L.W. Thewalt, "Luminescence in  $\text{Si}_{1-x}\text{Ge}_x$  heterostructures," *Mat. Res. Soc. Spr. Mtg.*, San Francisco, CA (1995).
11. C.W. Liu, A. St. Amour, J.C. Sturm, Y. Lacroix, and M.L.W. Thewalt, "Defect-free band-edge photoluminescence in  $\text{Si}_{1-x-y}\text{Ge}_x\text{C}_y$  strained layers grown by

- rapid thermal chemical vapor deposition," *Mat. Res. Soc. Spr. Mtg.*, San Francisco, CA (1995).
12. L.D. Lanzerotti, A. St. Amour, and J.C. Sturm, "Si/Si<sub>1-x-y</sub>Ge<sub>x</sub>C<sub>y</sub>/Si heterojunction bipolar transistors," *Int. Elec. Dev. Mtg.*, San Francisco, CA (1994).
  13. A. St. Amour, J.C. Sturm, Y. Lacroix, and M.L.W. Thewalt, "Silicon surface passivation control of high-temperature photoluminescence in Si/Si<sub>1-x</sub>Ge<sub>x</sub>/Si quantum wells," *IEEE Semi. Inter. Spec. Conf.*, San Diego, CA (1994).
  14. J.C. Sturm, A. St. Amour, S.L. Clark, Y. Lacroix, and M.L.W. Thewalt, "MBE-like deep photoluminescence in CVD Si/Si<sub>1-x</sub>Ge<sub>x</sub>/Si quantum wells created by ion implantation and annealing," *Elec. Mat. Conf.*, Boulder, CO (1994).
  15. C.W. Liu, A. St. Amour, and J.C. Sturm, "Low temperature chemical vapor deposition of Si<sub>1-x-y</sub>Ge<sub>x</sub>C<sub>y</sub> alloys on (100) Si substrates," *Elec. Mat. Conf.*, Boulder, CO (1994).
  16. A. St. Amour and J.C. Sturm, "Deposition of monolayer-scale Ge/Si heterostructures by rapid thermal chemical vapor deposition," *Mat. Res. Soc. Spr. Mtg.*, San Francisco, CA (1994).
  17. (invited) J.C. Sturm, X. Xiao, Q. Mi, A. St. Amour, L.C. Lenchyshyn, and M.L.W. Thewalt, "Opto-electronic applications of Si<sub>1-x</sub>Ge<sub>x</sub> heterostructures," *Int. Conf. Solid State Dev. Mat.* (1993) Makuhari, Japan.
  18. (invited) J.C. Sturm, X. Xiao, Q. Mi, C.W. Liu, A. St. Amour, Z. Matutinovic-Krstelj, L.C. Lenchyshyn, and M.L.W. Thewalt, "Photoluminescence and electroluminescence processes in Si/Si<sub>1-x</sub>Ge<sub>x</sub>/Si heterostructures grown by chemical vapor deposition," *European Mat. Res. Soc. Spr. Mtg.*, Strasbourg, France (1993).